



Search for electroweak production of charginos and neutralinos at $\sqrt{s} = 13$ TeV in final states containing hadronic decays of WW, WZ, or WH and missing transverse momentum

The CMS Collaboration*

CERN, Geneva, Switzerland

ARTICLE INFO

Article history:

Received 19 May 2022

Received in revised form 9 August 2022

Accepted 15 September 2022

Available online 13 May 2023

Editor: M. Doser

Keywords:

CMS

Gaugino

Electroweakino

Supersymmetry

ABSTRACT

This Letter presents a search for direct production of charginos and neutralinos via electroweak interactions. The results are based on data from proton-proton collisions at a center-of-mass energy of 13 TeV collected with the CMS detector at the LHC, corresponding to an integrated luminosity of 137 fb^{-1} . The search considers final states with large missing transverse momentum and pairs of hadronically decaying bosons WW, WZ, and WH, where H is the Higgs boson. These bosons are identified using novel algorithms. No significant excess of events is observed relative to the expectations from the standard model. Limits at the 95% confidence level are placed on the cross section for production of mass-degenerate wino-like supersymmetric particles $\tilde{\chi}_1^\pm$ and $\tilde{\chi}_2^0$, and mass-degenerate higgsino-like supersymmetric particles $\tilde{\chi}_1^\pm$, $\tilde{\chi}_2^0$, and $\tilde{\chi}_3^0$. In the limit of a nearly-massless lightest supersymmetric particle $\tilde{\chi}_1^0$, wino-like particles with masses up to 870 and 960 GeV are excluded in the cases of $\tilde{\chi}_2^0 \rightarrow Z\tilde{\chi}_1^0$ and $\tilde{\chi}_2^0 \rightarrow H\tilde{\chi}_1^0$, respectively, and higgsino-like particles are excluded between 300 and 650 GeV.

© 2022 The Author(s). Published by Elsevier B.V. This is an open access article under the CC BY license (<http://creativecommons.org/licenses/by/4.0/>). Funded by SCOAP³.

1. Introduction

Supersymmetry (SUSY) [1–10] proposes to extend the standard model (SM) of particle physics by the addition of a new symmetry. This new symmetry requires that, for each boson (fermion) in the SM, there is also a fermionic (bosonic) superpartner, also called a “sparticle”. SUSY can naturally predict cancellations of large radiative corrections to the Higgs boson (H) mass if some sparticles are not too heavy [11]. Recent work [12,13] suggests that strongly interacting sparticles significantly heavier than current bounds [14–28] are consistent with a natural theory [11]. Contrastingly, charginos and neutralinos are still expected to be lighter than ~ 1 TeV, with the lightest having a mass close to that of the Higgs boson. This suggests that the hunt for TeV-scale charginos and neutralinos is the next proving ground for natural SUSY.

In this Letter, we present a search for direct electroweak production of sparticles at the CERN LHC. The superpartners of the gauge bosons of the unbroken SU(2) and U(1) symmetries and the superpartners of the Higgs bosons (the winos, bino, and higgsinos, respectively) mix to form two chargino ($\tilde{\chi}_i^\pm$ with $i = 1, 2$) and four

neutralino ($\tilde{\chi}_i^0$ with $i = 1, 2, 3, 4$) mass eigenstates, where i is in order of increasing mass. In the case where the mass mixing of the charginos and neutralinos is nearly diagonal, each of the mass eigenstates is identified as bino-, wino-, or higgsino-like, depending on the dominant contribution [10].

We search for direct production of wino-like charginos and neutralinos ($\tilde{\chi}_1^\pm$ and $\tilde{\chi}_2^0$) or higgsino-like charginos and neutralinos ($\tilde{\chi}_1^\pm$, $\tilde{\chi}_2^0$, and $\tilde{\chi}_3^0$). We assume that the superpartners of the SM leptons are much heavier than the charginos and neutralinos. As such, decays of wino- or higgsino-like charginos and neutralinos proceed through W, Z, and Higgs bosons.

In this search, we assume that R -parity [29] is conserved and that the lightest neutralino is a bino-like $\tilde{\chi}_1^0$ that is stable and will escape the detector unobserved. Such a $\tilde{\chi}_1^0$ would be a viable candidate for weakly-interacting massive particle dark matter. We explore four signal regions, which target three prominent signatures when the scalar sparticles are very heavy: WW, WZ, or WH, together with a large transverse momentum imbalance.

At the LHC, several searches for direct chargino-neutralino and chargino-pair production in these channels have been performed by the ATLAS [30–38] and CMS [39–45] Collaborations. Most of these searches have been performed in events with at least one lepton. The present search is performed in fully hadronic final

* E-mail address: cms-publication-committee-chair@cern.ch.

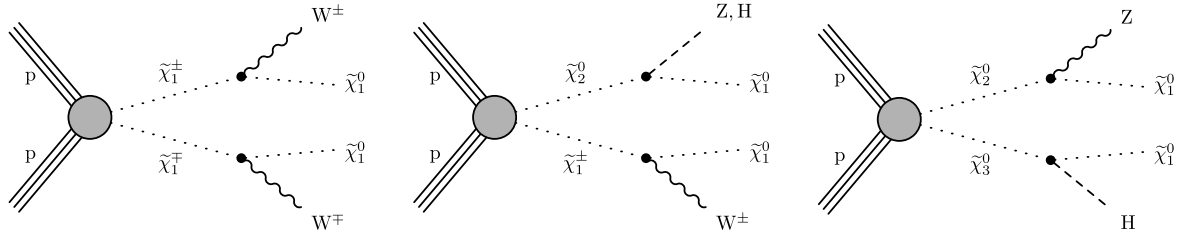


Fig. 1. Diagram for the production of $\tilde{\chi}_1^\pm\tilde{\chi}_1^\mp$ with the $\tilde{\chi}_1^\pm$ decaying to a W boson and $\tilde{\chi}_1^0$ (left). In the $\tilde{\chi}_1^\pm\tilde{\chi}_2^0$ production diagram (middle) the $\tilde{\chi}_1^\pm$ decays to a W boson and the $\tilde{\chi}_2^0$ decays to either a Z boson or a Higgs boson and $\tilde{\chi}_1^0$. In the case of $\tilde{\chi}_2^0\tilde{\chi}_3^0$ production (right) the $\tilde{\chi}_2^0$ and $\tilde{\chi}_3^0$ decay to a Z boson and Higgs boson, respectively, along with a $\tilde{\chi}_1^0$ each.

states, which feature larger branching fractions but larger backgrounds. Previous searches in fully hadronic final states have been performed for electroweak production of SUSY in the di-Higgs and other diboson channels by the ATLAS [37,46] and CMS [47,48] Collaborations. In this search we utilize machine learning algorithms to identify hadronically decaying high transverse momentum (p_T) W, Z, and Higgs bosons reconstructed as large-radius jets [49]. The search uses a sample of LHC proton-proton (pp) collisions at $\sqrt{s} = 13$ TeV collected by the CMS experiment between 2016 and 2018, corresponding to an integrated luminosity of 137 fb^{-1} . Tabulated results are provided in the HEPData record for this search [50].

2. Simulated event samples

Simulations of SM processes are used for optimizing selection criteria and computing several correction factors. These factors are used to predict the rates of SM backgrounds based on observations in various control regions. The production of $t\bar{t}$ + jets, W + jets, Z + jets, Drell-Yan, and quantum chromodynamics (QCD) multijet events is simulated at leading order (LO) using the MADGRAPH5_amc@NLO (2.2.2 for 2016 and 2.4.2 for 2017–2018) generator [51]. The $t\bar{t}$ + jets events are simulated with up to three additional partons at the matrix-element level, while the other samples are simulated with up to four additional partons at the matrix-element level. Single top quark events for all channels are modeled at next-to-leading order (NLO) in perturbative QCD. The MADGRAPH5_amc@NLO generator is used for s-channel production of single top quark events, while POWHEG v1.0 (v2.0) [52–56] is used to simulate t-channel and associated tW production for 2016 (2017–2018). Additional small backgrounds, such as $t\bar{t}$ produced in association with one or more SM bosons, are similarly produced at NLO with either MADGRAPH5_amc@NLO or POWHEG [57–59]. Events for 2016 (2017–2018) are generated using the NNPDF 3.0 (3.1) [60, 61] set of parton distribution functions (PDFs). Parton showering and fragmentation are performed using the PYTHIA 8.2 [62] program with the underlying event models detailed in Refs. [63,64]. The detector simulation is performed with GEANT4 [65]. Normalization of the simulated background samples is performed using the most accurate cross section calculations available [51,55,56,66–79], which typically correspond to NLO or next-to-NLO accuracy. Samples that are simulated at NLO with MADGRAPH5_amc@NLO adopt the FxFx scheme [80] for matching partons from the matrix-element calculation to those from parton showers. Samples simulated at LO adopt the MLM scheme [81] for the same purpose.

Signal events are generated with the MADGRAPH5_amc@NLO generator at LO precision in a similar manner to the SM backgrounds, with up to two additional partons at the matrix-element level. The detector simulation of signal samples is performed with the CMS fast simulation package [82,83]. The signal samples are corrected for differences with respect to the GEANT4-based simulation. Both the SM background samples and the signal samples are generated with nominal distributions of additional pp interactions per bunch crossing, referred to as pileup, which are then rescaled

to match the observed pileup distribution. The cross sections used for normalizing the signal yields are computed at NLO plus next-to-leading logarithmic precision [84–88].

We interpret our results in terms of simplified models [89–93] with the assumption that a chargino pair $\tilde{\chi}_1^\pm\tilde{\chi}_1^\mp$ or a chargino-neutralino pair $\tilde{\chi}_1^\pm\tilde{\chi}_2^0$ is produced. In the simplified model scenarios, the chargino always decays to a W boson and the $\tilde{\chi}_1^0$, while the neutralinos decay 100% of the time to either a Z or Higgs boson plus the $\tilde{\chi}_1^0$, where the $\tilde{\chi}_1^0$ is assumed to be the lightest supersymmetric particle (LSP), as depicted in Fig. 1. The simplified models are “TChiWW”, $\tilde{\chi}_1^\pm\tilde{\chi}_1^\mp$ production with $\tilde{\chi}_1^\pm$ decaying to a W boson and $\tilde{\chi}_1^0$; “TChiWZ”, $\tilde{\chi}_1^\pm\tilde{\chi}_2^0$ production with $\tilde{\chi}_2^0$ decaying to a Z boson and $\tilde{\chi}_1^0$; and “TChiWH”, $\tilde{\chi}_1^\pm\tilde{\chi}_2^0$ production with $\tilde{\chi}_2^0$ decaying to a Higgs boson and $\tilde{\chi}_1^0$. In the TChiWZ and TChiWH scenarios, the $\tilde{\chi}_1^\pm$ and $\tilde{\chi}_2^0$ are the mass-degenerate next-to-lightest supersymmetric particles (NLSPs), while in the TChiWW scenario, the $\tilde{\chi}_1^\pm$ is the NLSP. For these scenarios, we assume the $\tilde{\chi}_1^\pm$ and $\tilde{\chi}_2^0$ to be purely wino-like.

In addition to these simplified models, we also consider two more specific scenarios in which all of the winos or all of the higgsinos are mass degenerate, which we refer to as the wino- and higgsino-like NLSP scenarios. For the wino-like NLSP scenario, we assume a mass-degenerate $\tilde{\chi}_1^\pm\tilde{\chi}_2^0$ pair with a lighter bino-like $\tilde{\chi}_1^0$ as the LSP. In this scenario, both $\tilde{\chi}_1^\pm\tilde{\chi}_1^\mp$ and $\tilde{\chi}_1^\pm\tilde{\chi}_2^0$ production are expected and would contribute to the targeted signatures, so these two production processes are combined and searched for simultaneously. We consider two options for the decay of the $\tilde{\chi}_2^0$: either $\tilde{\chi}_2^0 \rightarrow Z\tilde{\chi}_1^0$ or $\tilde{\chi}_2^0 \rightarrow H\tilde{\chi}_1^0$, with 100% branching fraction in each case. For the higgsino-like NLSP scenario, we assume mass-degenerate $\tilde{\chi}_1^\pm$, $\tilde{\chi}_2^0$, and $\tilde{\chi}_3^0$ with a lighter bino-like $\tilde{\chi}_1^0$. In this scenario, the production of $\tilde{\chi}_1^\pm\tilde{\chi}_1^\mp$, $\tilde{\chi}_1^\pm\tilde{\chi}_2^0$, $\tilde{\chi}_1^\pm\tilde{\chi}_3^0$, and $\tilde{\chi}_2^0\tilde{\chi}_3^0$ are combined and searched for simultaneously. We assume 100% branching fractions of $\tilde{\chi}_2^0 \rightarrow Z\tilde{\chi}_1^0$ and $\tilde{\chi}_3^0 \rightarrow H\tilde{\chi}_1^0$ as expected for scenarios with $\tan\beta \sim 1$ [94,95]. We consider signal events with WW, WZ, WH, or ZH and large p_T^{miss} . The WW, WZ, and WH events arise from $\tilde{\chi}_1^\pm\tilde{\chi}_1^\mp$, $\tilde{\chi}_1^\pm\tilde{\chi}_2^0$, or $\tilde{\chi}_1^\pm\tilde{\chi}_3^0$ production. The ZH events arise from $\tilde{\chi}_2^0\tilde{\chi}_3^0$ production as shown in Fig. 1 (right). All the other sparticles are assumed to be too heavy to affect the production of charginos and neutralinos [86,87].

3. The CMS detector and event reconstruction

A detailed description of the CMS detector, together with a definition of the coordinate system used and the relevant kinematic variables, can be found in Ref. [96]. Briefly, a superconducting solenoid of 6 m internal diameter provides a magnetic field of 3.8 T. Within the solenoid volume are a silicon pixel and strip tracker covering pseudorapidity $|\eta| < 2.5$, a lead tungstate crystal electromagnetic calorimeter, and a brass and scintillator hadron calorimeter, each composed of a barrel and two endcap sections and covering $|\eta| < 3$. Forward calorimeters extend the pseudora-

pidity coverage to include $3 < |\eta| < 5.2$. Muons are detected in gas-ionization chambers embedded in the steel flux-return yoke outside the solenoid.

The particle-flow (PF) algorithm [97] combines all detector subsystems to identify and reconstruct charged and neutral hadrons, photons, electrons, and muons. This analysis utilizes PF jets, which are produced by clustering PF candidates into anti- k_T [98,99] jets. We utilize two jet collections in which the clustering size is either 0.4 (AK4 jets) or 0.8 (AK8 jets). The latter is well-suited for reconstructing hadronic decays of W, Z, and Higgs bosons with $p_T > 200$ GeV. We correct the jets for pileup effects [100,101] and the jet energy scale [102]. The AK8 jet mass m_J is calculated using the soft-drop algorithm [103]. We consider only AK4 jets with $p_T > 30$ GeV and $|\eta| < 2.4$ and AK8 jets with $p_T > 200$ GeV and $|\eta| < 2$ that satisfy a set of quality criteria to eliminate jets from spurious sources, such as electronics noise [100].

The variable \vec{p}_T^{miss} is defined as the negative vector sum of \vec{p}_T for all PF candidates, and its magnitude is denoted by p_T^{miss} . Known detector effects are accounted for by adjusting p_T^{miss} for jet energy corrections [104]. A set of quality criteria is used to identify and eliminate events in which detector noise, inoperable calorimeter cells, beam halo, and other effects mimic p_T^{miss} [104].

The identification of jets originating from a bottom quark (b tagging) is performed by applying a version of the combined secondary vertex algorithm that utilizes deep-learning techniques [105]. For the medium working point utilized in this search, the efficiency of tagging b jets with $p_T > 30$ GeV, as measured in $t\bar{t}$ events, is about 68%; the probability of misidentifying jets arising from the hadronization of a charm quark is roughly 12% and for jets from a light-flavor quark or a gluon it is roughly 1%.

The lepton content of events is used to separate the fully hadronic signal samples from the single-lepton control samples, as described in Sections 4 and 5. We require electron and muon candidates [106,107] to have $p_T > 10$ GeV and to lie within $|\eta| < 2.5$ for electrons and $|\eta| < 2.4$ for muons. Electron candidates are required to satisfy the “veto” requirements described in Ref. [106], and muon candidates are required to satisfy the “medium” requirements described in Ref. [107]. We also impose isolation requirements on electron and muon candidates to suppress those arising from jets erroneously identified as leptons, as well as genuine leptons from hadron decays, using the same criteria as in Refs. [22,108]. To recover electrons or muons that fail the identification requirements, as well as τ leptons via their one-prong hadronic decays, we make use of isolated tracks. Isolated tracks are required to satisfy $|\eta| < 2.4$ and $p_T > 5$ GeV for PF electrons and muons, and $p_T > 10$ GeV for PF hadrons [22].

Photon candidates, which are only used to remove events from the data set as described in Section 4, are required to have $p_T > 100$ GeV and $|\eta| < 2.4$ and to be isolated from charged hadrons, neutral hadrons, and electromagnetic particles [109].

Candidate AK8 jets consistent with the decay and subsequent fragmentation and hadronization of heavy SM bosons are identified using a deep neural network (DNN). The DNN is designed to classify AK8 jets arising from hadronically decaying particles of five main categories: W, Z, H, t, and “other”. Jets are further classified into subcategories according to their likelihood of originating from specific decays of these unstable particles, e.g., $Z(b\bar{b})$, $Z(c\bar{c})$, etc. The architecture of the DNN and details of its training can be found in Ref. [49]. Each classification has a corresponding score that is used to develop jet taggers.

In this analysis, three jet taggers, which were developed from these classifiers, are used to categorize AK8 jets: the W tagger, the V tagger, and the $b\bar{b}$ tagger. These taggers are non-exclusive, i.e., a single AK8 jet may be tagged by any, all, or none of the three taggers. Each tagger involves the DNN and the jet mass. The W tagger identifies jets consistent with a $W(q\bar{q}')$ decay by their

mass ($65 < m_J < 105$ GeV) and a DNN score optimized for distinguishing between hadronic W boson decays and QCD jets. The V tagger identifies jets consistent with a $W(q\bar{q}')$ or $Z(q\bar{q})$ decay by their mass ($65 < m_J < 105$ GeV) and a DNN score optimized in a similar manner to the W tagger, but utilizing adversarial training [110] to decorrelate the DNN score and the jet mass, which allows the V tagger to be sensitive to the hadronic decays of both the W and Z bosons despite a higher misidentification rate. The $b\bar{b}$ tagger identifies AK8 jets consistent with a $Z(b\bar{b})$ or $H(b\bar{b})$ decay by their mass ($75 < m_J < 140$ GeV) and a DNN score optimized for identifying Lorentz-boosted $b\bar{b}$ topologies. The $b\bar{b}$ tagger also utilizes adversarial training to decorrelate the DNN score and the jet mass. The $b\bar{b}$ tagger has an efficiency of about 54% for jets with $p_T > 300$ GeV originating from Higgs or Z bosons decaying into $b\bar{b}$, and a misidentification rate of roughly 2.5% for QCD jets. Similarly, the W tagger has an efficiency of about 41% for jets arising from hadronic W boson decays and a misidentification rate of roughly 1%, and the V tagger has an efficiency of about 45% for tagging hadronic W and Z boson decays and a misidentification rate of roughly 2.5%.

4. Triggers and event selection

Candidate events are recorded based on a trigger [111] that requires p_T^{miss} to be larger than a time-dependent threshold that varies between 90 and 140 GeV. The efficiency of these triggers is measured using a separate data set in which events are recorded based on the requirement that a single electron or single muon is reconstructed. For p_T^{miss} of about 200 GeV, which is the minimum p_T^{miss} used in this search, the trigger efficiency is found to be 95, 78, and 74% for the 2016, 2017, and 2018 data-taking periods, respectively. This variation in the trigger efficiency is caused by the changes in the trigger threshold over time, but the efficiency rises above 98% for $p_T^{\text{miss}} > 270$ GeV for all years. When computing event yields, parameterizations of these efficiencies are used to correct simulations. For ancillary measurements of jet tagging rates in the data, a combination of single-lepton and dilepton triggers is used.

All events in our signal regions (SRs) are required to satisfy a common set of baseline selection criteria. Each event is required to have a primary vertex [112] and no isolated leptons, isolated photons, or isolated tracks. Leptons, in particular, typically arise from a W boson decay, which constitutes a major background. The requirement of no leptons in our SRs makes this analysis orthogonal to other searches targeting common signals in final states that include leptons [39–43]. Events containing isolated tracks are only removed from the data set if the transverse mass based on the track satisfies $m_T = \sqrt{2p_T p_T^{\text{miss}}(1 - \cos \Delta\phi)} < 100$ GeV, where $\Delta\phi$ refers to the azimuthal separation between the track and \vec{p}_T^{miss} directions. Low m_T is typical of tracks from $W \rightarrow \ell\nu$ decays but less common in signal events with isolated tracks. Events are required to have $p_T^{\text{miss}} > 200$ GeV and $H_T > 300$ GeV, where H_T is defined as the scalar sum of p_T for all AK4 jets which satisfy the kinematic and quality criteria mentioned in Section 3. Large p_T^{miss} and H_T values are typical of chargino and neutralino production when a high-momentum boson is present. Signal events typically have two AK8 jets and four AK4 jets (note that AK4 jets may overlap AK8 jets); accordingly we require at least two AK8 jets and 2–6 (inclusive) AK4 jets. We also impose requirements on the azimuthal angle $\Delta\phi_i$ between \vec{p}_T^{miss} and each of the four highest p_T AK4 jets, where the subscript i refers to the p_T ordering of the jets. Each event must satisfy $\Delta\phi_{1,2,3,4} > 1.5, 0.5, 0.3$, and 0.3 . Events must satisfy $\Delta\Phi_{1,2} > 1.5$ and 0.5 , where $\Delta\Phi_i$ is defined analogously to $\Delta\phi_i$ using the two highest p_T AK8 jets. These requirements on azimuthal angles suppress the background from QCD multijet events, for which \vec{p}_T^{miss} is usually aligned along a jet direction. Within this

Table 1

Summary of tagging requirements for the b-veto SR and CRs. Each of these regions includes the baseline selection described in Section 4 and requires zero b-tagged AK4 jets and at least two AK8 jets satisfying $65 < m_j < 105$ GeV. The SR and CRs are described in detail in Sections 4.1 and 5.1, respectively. The W and V taggers are described in Section 3.

Region	Requirements
b-veto SR	≥ 1 V-tagged jet ≥ 1 W-tagged jet ≥ 2 V- or W-tagged jets
b-veto 0-tag CR	0 V-tagged jets 0 W-tagged jets
b-veto 1-tag CR	1 V-tagged jet 0 other W-tagged jets

baseline phase space, four SRs are defined. One SR, which we refer to as the b-veto region, requires zero b-tagged AK4 jets ($n_b = 0$) and targets signal events in which SM bosons decay to light-flavor quarks. The remaining three SRs, which we refer to as the b-tag regions, require at least one b-tagged AK4 jet ($n_b \geq 1$) and target signal events in which at least one SM boson decays to $b\bar{b}$. In addition to these SRs, we also define several control regions (CRs), which are used to help constrain the background estimates, as described in Section 5.

4.1. The b-veto search region

The b-veto SR seeks to isolate events that are consistent with the production of WW or WZ pairs of bosons, along with a large p_T^{miss} . In addition to the baseline event selection described above, the b-veto SR requires that at least two AK8 jets satisfy $65 < m_j < 105$ GeV. At least one AK8 jet must be W tagged, and at least one other AK8 jet must be V tagged, as described in Section 3. A summary of the b-veto SR requirements is shown in Table 1. The b-veto SR is further subdivided into nine bins of p_T^{miss} . The lower p_T^{miss} bin boundaries are 200, 250, 300, 350, 400, 450, 500, 600, and 800 GeV.

The main background in the b-veto SR arises from $W/Z + \text{jets}$ production with $W \rightarrow \ell\nu$ or $Z \rightarrow \nu\bar{\nu}$. The $W \rightarrow \ell\nu$ background is substantially reduced by requiring the number of reconstructed charged leptons and isolated tracks to be zero. These events still satisfy the event selection criteria when the charged lepton lies outside the lepton acceptance, is not reconstructed, or is not isolated. In $W/Z + \text{jets}$ background events, both W- and V-tagged AK8 jets arise from misidentification of jets not originating from hadronic W or Z boson decays. These events together with background events arising from QCD multijet production do not contain any resonance reconstructed as a single AK8 jet, and are referred to as the “0-res” background.

The next largest background contributions come from $t\bar{t}$, single top quark, and diboson production. These events typically have one leptonically decaying vector boson and one hadronically decaying vector boson. Therefore, one W- or V-tagged AK8 jet arises from a hadronic W or Z boson decay, and the other tag arises from misidentification. We refer to these backgrounds, which contain only one resonance reconstructed as a single AK8 jet, as the “1-res” backgrounds. The remaining minor background contributions, which constitute less than 10% of the expected event yield in any p_T^{miss} bin of the SR, are expected from rare processes such as triboson production and $t\bar{t}$ pairs produced in association with a W, Z, or Higgs boson.

The m_j distribution of V-tagged jets for signal, expected SM backgrounds, and observed event yields in the b-veto SR is shown in Fig. 2 (upper), in which the mass requirement of the V tagger

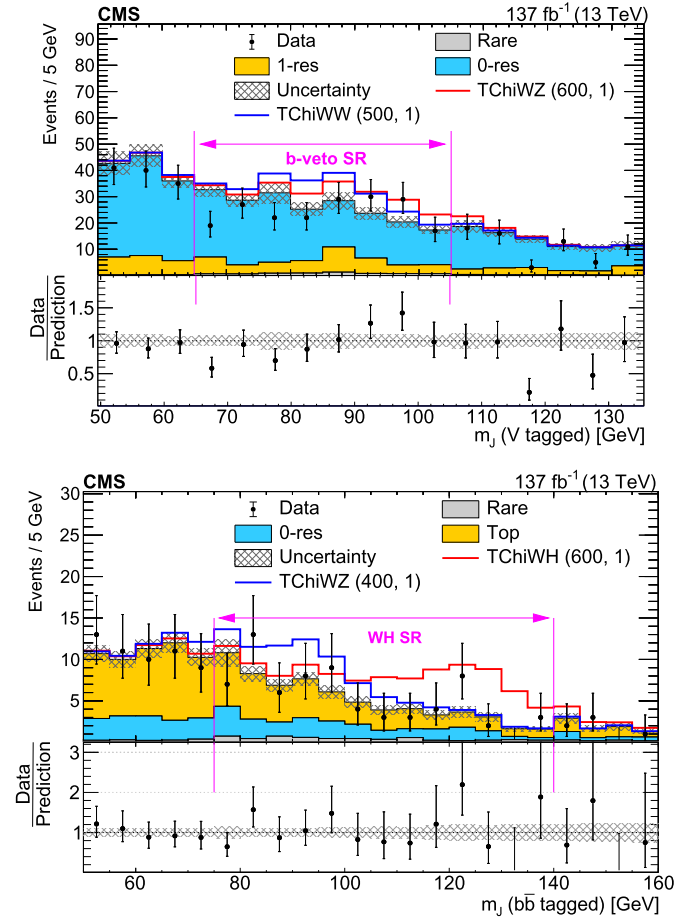


Fig. 2. Distributions of the jet mass for V-tagged AK8 jets in the b-veto SR (upper) and $b\bar{b}$ -tagged AK8 jets in the WH SR (lower). The jet mass requirements for the V and $b\bar{b}$ taggers have been loosened in these figures. The filled histograms show the SM background simulation, scaled such that the yield within the SR matches the total SM background predictions. The open histograms show the sum of the scaled SM background simulations and of the expectations for selected signal models, which are denoted in the legend by the name of the model followed by the assumed masses of the NLSB and LSP in GeV. The observed event yields are indicated by black markers. The hatched gray bands correspond to the statistical uncertainties in the SM predictions, but no systematic uncertainties are included.

has been loosened to show the behavior of the signal and backgrounds in both the tagged regions and the sidebands. In some events, there are multiple V-tagged jets, some of which could also be W tagged. In such events, the jet that is both W and V tagged and has the highest W tagger DNN score is ignored, and the V-tagged jet with the highest V tagger DNN score among the remaining jets is plotted. The simulated event yields are scaled such that the yield within the SR matches our total SM background predictions, which will be described in Section 5. The distributions for the TChiWZ and TChiWW signals show peaks in the region of 65–105 GeV, corresponding to the mass requirement of the V tagger.

4.2. The b-tag search regions

To maximize our acceptance of signal events, we define three SRs for events containing at least one b-tagged AK4 jet. These SRs are defined in terms of the numbers of “W boson candidates” and “Higgs boson candidates”, which are AK8 jets selected according to m_j and according to their proximity to a b-tagged AK4 jet. An AK8 jet is said to contain a b-tagged AK4 jet if the event includes at least one b-tagged AK4 jet that satisfies

Table 2

Summary of tagging requirements for the b-tag SRs and CRs. Each of these regions includes the baseline requirements described in Section 4 and requires at least one b-tagged AK4 jet and at least two AK8 jets. The SRs and CRs are described in detail in Sections 4.2 and 5.2, respectively. The $b\bar{b}$ and W taggers are described in Section 3, and the definitions of W and Higgs boson candidates are given in Section 4.2. In addition to the six regions described in this table, the b-tag predictions also use six single-lepton CRs that are identical except that exactly one charged lepton is required. A dash (–) indicates that no requirement is imposed.

	W boson candidate		Higgs boson candidate	
	W tagged	not W tagged	$b\bar{b}$ tagged	not $b\bar{b}$ tagged
WH SR	≥ 1	–	≥ 1	–
W SR	≥ 1	–	0	–
H SR	0	–	≥ 1	–
WH antitag CR	0	≥ 1	0	≥ 1
W antitag CR	0	≥ 1	0	0
H antitag CR	0	0	0	≥ 1

$\Delta R(\text{b jet, AK8 jet}) < 0.8$, where $\Delta R = \sqrt{(\Delta\eta)^2 + (\Delta\phi)^2}$ is the distance in the pseudorapidity-azimuth plane. A W boson candidate is any AK8 jet that lies in the W/Z mass window $65 < m_j < 105$ GeV and does not contain a b-tagged jet. Similarly, a Higgs boson candidate is any AK8 jet that lies in the Z/H mass window $75 < m_j < 140$ GeV and contains at least one b-tagged jet. These two classes of AK8 jets do not overlap, but not every AK8 jet falls into either class. We further subdivide these classes based on jet tagging. The W tagger is used to divide W boson candidates into tagged and untagged subcategories, and the $b\bar{b}$ tagger is similarly used to divide Higgs boson candidates into tagged and untagged subcategories.

The three SRs with b-tagged jets are referred to as the WH, W, and H SRs. These SRs isolate events in which a WH, WZ, or ZH pair of bosons is produced with large p_T^{miss} . The WH SR requires at least one tagged W boson candidate and at least one tagged Higgs boson candidate. The W SR requires at least one tagged W boson candidate and exactly zero tagged Higgs boson candidates, although untagged Higgs boson candidates are permitted. The H SR requires at least one tagged Higgs boson candidate and exactly zero tagged W boson candidates, but similarly imposes no requirement on untagged W boson candidates. These requirements are summarized in Table 2.

The SM backgrounds that contribute to the three b-tag SRs are top quark pair production, especially at low p_T^{miss} , and W/Z + jets events, especially at high p_T^{miss} . In all three b-tag SRs, there are small contributions from diboson and triboson production, as well as $t\bar{t}$ production in association with a W, Z, or Higgs boson. The backgrounds containing top quarks include a mixture of events with one and two resonances each reconstructed as a single AK8 jet, and so we refer to these backgrounds in the b-tag region as “top” rather than as “1-res”.

The b-tag SRs are also subdivided into bins of p_T^{miss} . The W and H SRs use the same p_T^{miss} binning as the b-veto SR. For the WH SR, the last two p_T^{miss} bins are merged because of the small expected number of events in the corresponding CRs.

The distribution of the Higgs boson candidate m_j for events in the WH SR for signal, expected SM backgrounds, and observed event yields is shown in Fig. 2 (lower), in which the Higgs boson candidate mass requirement has been loosened by ~ 20 GeV on either side to show the distribution both in and near the SR. The predicted yields from simulation are scaled such that the total SM background yields in the SR match the total prediction using the procedure described in Section 5. Distributions for the TChiWZ and TChiWH signals show peaks in the region of 75–140 GeV, corresponding to the Z and Higgs boson masses.

5. Background estimation

To constrain the contribution from the dominant SM processes in each of our SRs, several CRs are defined. Each CR has reduced contributions from signal processes and enhanced contributions from SM background processes. Most of our CRs isolate different background components by inverting various tagging requirements to select events with a misidentified boson. For the b-tag SRs, where backgrounds involving top quarks are more prominent, a combination of CRs with inverted tagging requirements and with one charged lepton is used.

5.1. Background estimation for the b-veto search region

The sum of 0- and 1-res background events in the b-veto SR is estimated simultaneously from two mutually-exclusive CRs. Both CRs require at least two AK8 jets that satisfy the WZ mass requirements. The 0-tag CR is defined by requiring that all AK8 jets satisfying the WZ mass requirements are neither W tagged nor V tagged. This CR is dominated by the 0-res background. The 1-tag CR requires exactly one V-tagged jet, and requires that all other AK8 jets that satisfy the WZ mass requirements are neither W tagged nor V tagged. The main contribution to the 1-tag CR also comes from the 0-res background, but this CR has increased contributions from the 1-res background compared to the 0-tag CR. The requirements for both b-veto CRs are summarized in Table 1.

The background yields in the b-veto SR are estimated using two sets of transfer factors derived from simulation, \mathcal{R}_i , defined as the ratio of the summed 0- and 1-res event yields in the SR divided by those in either the 0-tag (\mathcal{R}_0) or 1-tag CR (\mathcal{R}_1). The values of \mathcal{R}_i are computed separately for each p_T^{miss} bin and typically range between 0.2 and 0.3. The contributions of rare processes to the SR and CRs are taken from simulation with appropriate data-to-simulation corrections applied [49,102,105]. The total background prediction is given by

$$N_{\text{SR}}^{\text{pred}} = \mathcal{R}_i (N_{\text{CR}_i}^{\text{data}} - N_{\text{CR}_i, \text{rare}}^{\text{MC}}) + N_{\text{SR, rare}}^{\text{MC}},$$

where N denotes the number of events expected (or observed in data) in regions and from processes indicated by the superscripts and subscripts, $\mathcal{R}_i = N_{\text{SR, 0\&1-res}}^{\text{MC}} / N_{\text{CR}_i, 0\&1-res}^{\text{MC}}$, and CR_i is either the 0- or 1-tag CR. The final background predictions for the SR are determined by a simultaneous fit of the two CRs. The background composition of the 1-tag CR is very similar to the b-veto SR, while the signal contamination is smaller in the 0-tag CR. The level of signal contamination in the CRs depends on the choice of SUSY model and on the assumed NLSP and LSP masses. Both CRs are included in the fits to the data described in Section 7, and the signal contamination, although small, is taken into account in the fits. Using both CRs allows us to benefit from the varying background compositions and signal contamination levels.

The W and V tagging rates in simulation are corrected to match those measured in data. The corrections for jets matched to generator-level W bosons are obtained from a $t\bar{t}$ -enriched sample in which one of the W bosons from the top quark decays leptonically and the other decays hadronically [49]. The same corrections are also applied to jets matched to generator-level Z bosons. The corrections for misidentified jets are obtained from a sample of events with an $\ell^+\ell^-$ ($\ell = e, \mu$) pair and at least one AK8 jet. The W- or V-tagged jets in these events are dominated by misidentification. Uncertainties associated with the determination of these corrections are propagated to the final predictions.

Our b-veto background prediction method relies on the modeling of the AK8 jet W- and V-tagging efficiencies in simulation after the corrections described above are applied. Several validation regions (VRs) are defined to check how well the simulation models

the tagging efficiencies in the phase space close to our SR and CRs. For one set of VRs, events are required to satisfy the baseline event selection criteria except for the second AK8 jet requirement, and to have only one AK8 jet, which is W or V tagged. These VRs are referred to as the 1-jet W- and V-tag VRs, respectively. The predicted SM backgrounds, with the exception of the rare backgrounds, in each VR are based on an extrapolation from CRs defined by the inversion of the DNN requirement for the W or V tag compared to the corresponding VR. The predicted yields of the rare backgrounds are obtained directly from simulation, not via extrapolation from CRs. The predictions in these 1-jet VRs are found to be compatible with our observations.

Similar tests are also performed using events that satisfy the baseline event selection criteria including the requirement of having at least two AK8 jets but only one of them satisfying $65 < m_j < 105$ GeV. These events are orthogonal to events in any of b-veto SR and CRs, as the b-veto SR and CRs require at least two jets to satisfy $65 < m_j < 105$ GeV. We then require that only one AK8 jet is W or V tagged. These b-veto VRs are referred to as the 2-jet W- and V-tag VRs, respectively. Predictions of the background yields, with the exception of the rare backgrounds, are made by extrapolating from CRs defined by inversion of the tagging DNN requirement. As before the rare background yields are taken directly from simulation.

In the 2-jet W- and V-tag VRs, the observed event yields are higher than the SM background predictions, primarily in the intermediate- to high- p_T^{miss} region, which may be attributed to a dependence of the misidentification rate corrections on event topology or on AK8 jet multiplicity in this phase space. We correct the background predictions in the b-veto SR to account for these discrepancies. The correction from the W-tag VR is applied to the extrapolation from the 1-tag CR to the SR, and the corrections from the W- and V-tag CRs are both applied to the extrapolation from the 0-tag CR to the SR. The corrections obtained from the 2-jet W- and V-tag VRs range from 1.03 and 1.01 at low p_T^{miss} to 1.48 and 1.27 in the highest p_T^{miss} bin, respectively. The full size of these corrections is considered as a systematic uncertainty.

5.2. Background estimation for the b-tag search regions

For each of the three b-tag SRs, we define three sets of CRs, for a total of nine CRs. The first set, the antitag CRs, inverts the boson tagging requirements of the corresponding SRs. In the antitag CRs, every Higgs boson candidate must not be $b\bar{b}$ tagged, and every W boson candidate must not be W tagged. Otherwise, the definitions of the WH, W, and H antitag CRs, which are summarized in Table 2, are identical to the corresponding SRs. The antitag CRs are enhanced in W/Z + jets but still have contributions from events containing top quarks.

The two remaining sets of CRs are defined identically to the SRs and antitag CRs but require exactly one lepton, i.e., there is a set of three single-lepton (1ℓ) tagged CRs and a set of three 1ℓ antitag CRs. The 1ℓ CRs feature enhanced rates of top quark pair production. A summary of the selection for each SR and corresponding CR is given in Table 2. All of the SRs and CRs are mutually non-overlapping.

The 1ℓ CRs are used to constrain the estimates of top quark backgrounds in the SRs and zero-lepton antitag CRs, while the antitag CRs are used to constrain the estimates of the 0-res backgrounds in the SRs and tagged CRs. The signal contamination in the b-tag CRs is negligible in most of the CRs for most signal models.

The 1ℓ CRs are dominated by top quark pair production, with small contributions from W + jets and even smaller contributions from single top quark production and $t\bar{t}H$. A transfer factor, $\mathcal{R}_{0\ell/1\ell}$,

is used to provide an estimate of the number of top quark background events in either the SR or the 0ℓ antitag CR, where 0ℓ refers to the SRs and the antitag CRs with zero leptons. The values of $\mathcal{R}_{0\ell/1\ell}$ are computed from simulation, including all corrections to the lepton reconstruction efficiencies, b tagging efficiencies, and AK8 jet tagging efficiencies.

The predicted number of top quark background events in either the SR or the 0ℓ antitag CR is given by

$$N_{i,\text{top}}^{\text{pred},0\ell} = \frac{N_{i,\text{top}}^{\text{MC},0\ell}}{N_{i,\text{all}}^{\text{MC},1\ell}} N_i^{\text{data},1\ell} = \mathcal{R}_{0\ell/1\ell} N_i^{\text{data},1\ell}, \quad (1)$$

where N^{MC} denotes the number of events expected from simulation, N^{data} denotes the number of observed events, and N^{pred} denotes the number of events predicted via this method. Additionally, the subscript i denotes the tagging region, tag or antitag. The subscript "all" refers to all of the SM backgrounds, while "top" refers to only the top quark backgrounds.

A transfer factor \mathcal{R}_{tag} is used to constrain the 0-res event yields in the SR based on observations in the 0ℓ antitag CR. The value of \mathcal{R}_{tag} is computed using simulation and is the ratio of the number of 0-res events in the SR to the number of 0-res events in the 0ℓ antitag CR. This transfer factor does not include the top quark backgrounds, which are constrained separately via the 1ℓ CRs. The transfer factor is corrected for differences in tagging rates between simulation and data. Corrections are derived separately for W- and $b\bar{b}$ -tagged jets, and separately for misidentified and correctly tagged jets [49]. Corrections for misidentified jets are derived in a similar manner to the corrections used for the b-veto regions, using samples of Drell-Yan events and requiring $n_b = 1$. All uncertainties in the tagging and misidentification rate corrections are propagated to the final predictions.

Using \mathcal{R}_{tag} and the prediction of the top quark backgrounds described above, the predicted 0-res background contribution to the SR is given by

$$N_{0\text{-res}}^{\text{pred},0\ell} = \mathcal{R}_{\text{tag}} \left(N_{\text{antitag}}^{\text{data},0\ell} - N_{\text{antitag,top}}^{\text{pred},0\ell} - N_{\text{antitag,rare}}^{\text{MC},0\ell} \right), \quad (2)$$

where $N_{\text{antitag}}^{\text{data},0\ell}$ denotes the number of observed events in the 0ℓ antitag CR, $N_{\text{antitag,top}}^{\text{pred},0\ell}$ denotes the predicted number of top quark background events from Eq. (1), and $N_{\text{antitag,rare}}^{\text{MC},0\ell}$ denotes the number of rare background events, such as diboson and triboson events, expected from simulation.

The predictions of the top quark backgrounds and 0-res backgrounds are taken from Eqs. (1) and (2), while the prediction of the rare backgrounds is taken from simulation. These predictions are produced in each p_T^{miss} bin and in each SR independently. Each transfer factor is derived separately for each p_T^{miss} bin except for $\mathcal{R}_{0\ell/1\ell}$, whose values above $p_T^{\text{miss}} > 450$ (400) GeV are averaged in the W and H (WH) SRs.

The predictions of the SM backgrounds are tested in data using an orthogonal VR in which exactly one AK8 jet is required. This VR is used to test the simulation-derived transfer factors, misidentification scale factors, and simulation-based contamination terms in the CRs. Within the VR, two pseudo-SRs are defined in which the AK8 jet is W tagged or $b\bar{b}$ tagged, respectively. For each pseudo-SR, a 0ℓ antitag CR and 1ℓ tag and antitag CRs are defined for the background estimation. All transfer factors are rederived in the VR phase space. Predictions and observations in the pseudo-SRs are found to be statistically compatible.

6. Systematic uncertainties

For all SRs and CRs, the expected rate of signal and backgrounds is adjusted for known differences between data and simulation in

Table 3

The dominant systematic uncertainties and their effects on event yields (in %) in various SRs. For the 0- and 1-res backgrounds in the b-veto SR, uncertainties are presented separately depending on the CR region used for the estimation. A dash (-) indicates that the source of uncertainty is not applicable.

Source	b veto				b tag			
	0- and 1-res bkg.		Rare	Signal	Top quark	0-res	Rare	Signal
	0-tag CR	1-tag CR						
Integr. luminosity	-	-	1.6	1.6	-	-	1.6	1.6
CR data size	6-71	5-50	-	-	3-100	2-35	-	-
MC sample size	8-25	8-30	14-24	2-5	2-28	3-40	4-27	2-5
μ_R and μ_F	1.2	0.4	8	<5	2-10	0.5	11	<5
Trigger efficiency	-	-	2-3	2-3	-	-	2-3	2-3
b-tag correction	<1	<1	<1	1	1	<3	<3	2-3
bb-tag correction	-	-	-	-	-	4	2-7	4
W-tag correction	12-28	6-22	11-15	15	1	9	7	9
V-tag correction	7-15	2-10	1-4	2	-	-	-	-
W-tag nonclosure	3-48	3-48	-	-	-	-	-	-
V-tag nonclosure	1-27	-	-	-	-	-	-	-
1-res cross sections	2	4	-	-	-	-	-	-
Fast simulation	-	-	-	5	-	-	-	8

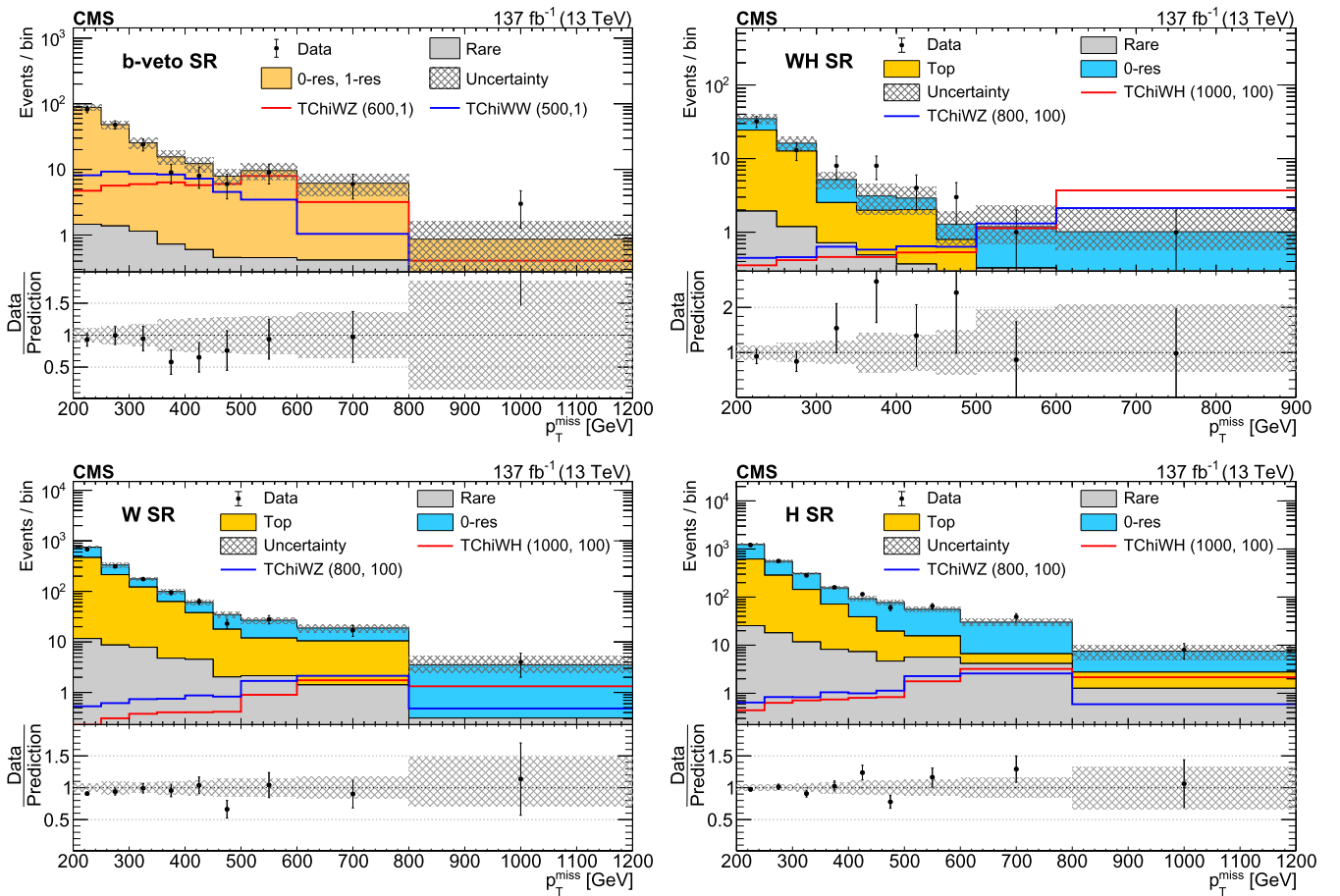


Fig. 3. SM background prediction vs. observation in the b-veto SR (upper left), the WH SR (upper right), the W SR (lower left), and the H SR (lower right). The filled stacked histograms show the SM background predictions from the fit to the data in the CRs under the background-only hypothesis. The superimposed open histograms show the expectations for selected signal models, which are denoted in the legend by the name of the model followed by the assumed masses of the NLSP and LSP in GeV. The observed event yields are indicated by black markers. The hatched gray band corresponds to the total uncertainty in the prediction.

the jet tagging rates (using the b, bb, W, and V taggers), lepton identification rates, and trigger efficiencies. Additional corrections are applied to the predicted signal yields to account for known differences between the GEANT4-based CMS detector simulation and the CMS fast simulation in the AK8 jet mass, W tagging, V tagging, bb tagging, b tagging, and p_T^{miss} . Uncertainties associated with the determination of these correction factors are propagated to the final yield estimates, as is the uncertainty in the integrated

luminosity [113–115]. Uncertainties related to the determination of the trigger efficiency are dominated by the limited size of the data sets in which we measure the trigger efficiency at high p_T^{miss} and by the differences between the efficiencies determined using two classes of events, namely events with one electron and events with one muon, at low p_T^{miss} . Uncertainties related to the corrections to the rates of jet misidentification are due to the limited size of our dilepton data sets. Uncertainties associated with the

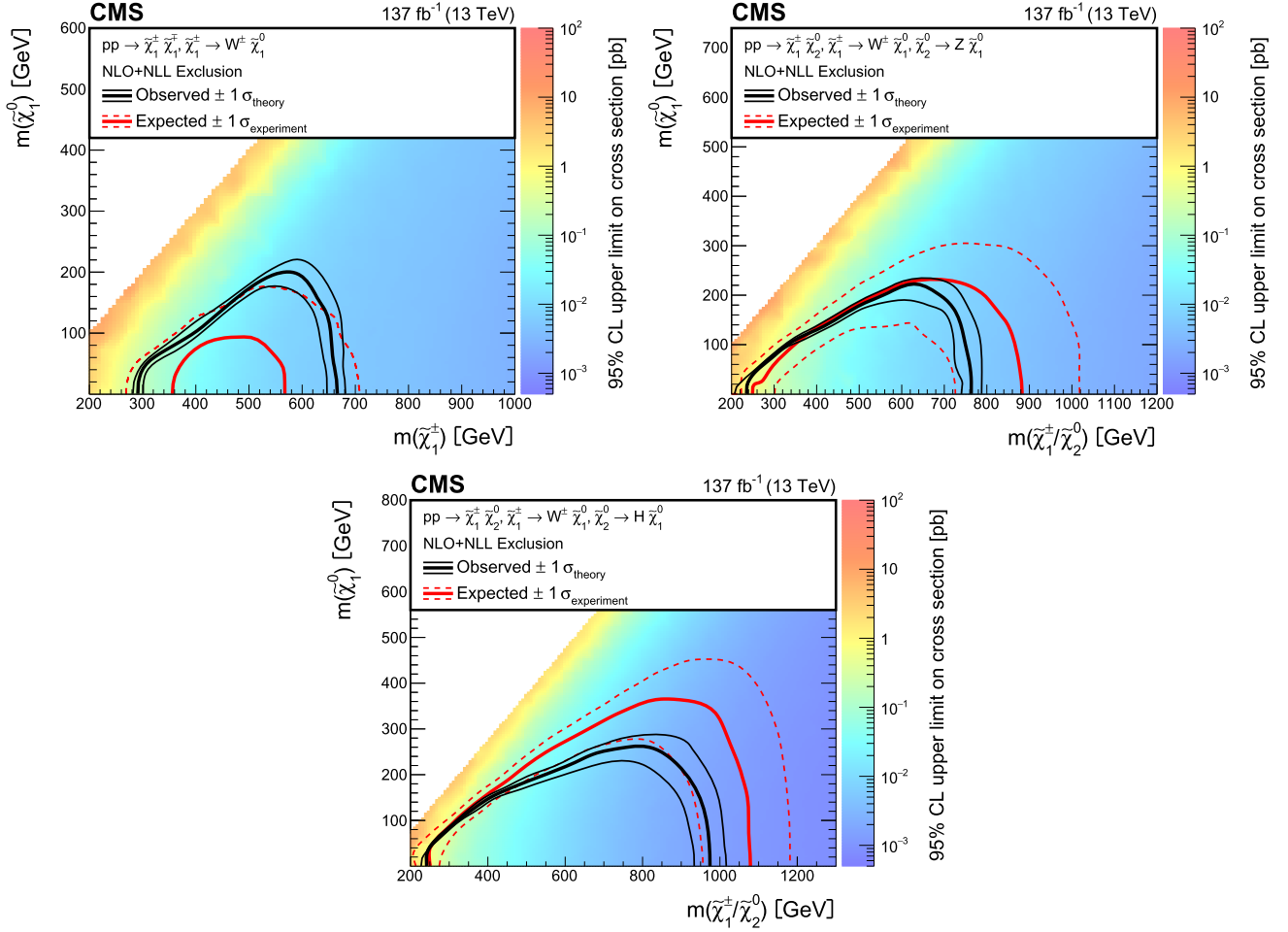


Fig. 4. The 95% CL upper limits on the production cross sections for $\tilde{\chi}_1^\pm \tilde{\chi}_1^\mp$ assuming that each $\tilde{\chi}_1^\pm$ decays to a W boson and $\tilde{\chi}_1^0$ (upper left, the TChiWW model) and $\tilde{\chi}_1^\pm \tilde{\chi}_2^0$ production assuming that the $\tilde{\chi}_1^\pm$ decays to a W boson and $\tilde{\chi}_1^0$ and that the $\tilde{\chi}_2^0$ decays to a Z boson and $\tilde{\chi}_1^0$ (upper right, the TChiWZ model) or that the $\tilde{\chi}_2^0$ decays to a Higgs boson and $\tilde{\chi}_1^0$ (lower, the TChiWH model). The black curves represent the observed exclusion contour and the change in this contour due to variation of these cross sections within their theoretical uncertainties (σ_{theory}). The red curves indicate the mean expected exclusion contour and the region containing 68% ($\pm 1\sigma_{\text{experiment}}$) of the expected exclusion limits under the background-only hypothesis. The mass exclusion limits are computed assuming wino-like cross sections.

lepton identification efficiency corrections and jet tagging rate corrections are detailed in Refs. [106,107] and [49,105], respectively. In this analysis, the W tagger is used to identify $W(q\bar{q}')$ decays, but some signal events with ZH and large $p_{\text{T}}^{\text{miss}}$ in the higgsino-like NLSP scenario enter the b-tag WH or W SRs when $Z(q\bar{q})$ decays are selected by the W tagger. The W tagger efficiency is lower for $Z(q\bar{q})$ decays than for $W(q\bar{q}')$ decays by 20–40% in simulation, but its performance is calibrated only for $W(q\bar{q}')$ decays and not for $Z(q\bar{q})$ decays in data. Therefore, additional uncertainties are applied when ZH signal events enter the b-tag WH or W SRs. Because the effect of these uncertainties on our results is small, we conservatively chose the size of the uncertainty to correspond to half the W tagger efficiency differences between $W(q\bar{q}')$ and $Z(q\bar{q})$ decays in simulation. The corrections to the jet tagging rates in the b-veto SR and CRs derived from the VRs described in Section 5.1 are treated as systematic uncertainties, and are referred to as the “nonclosure” uncertainties. The uncertainty in the top and diboson production cross sections [116–121] produces about a 4% effect on the b-veto \mathcal{R}_i . Additional uncertainties associated with the choice of the renormalization and factorization scales μ_{R} and μ_{F} were assessed by varying them independently up and down by a factor of 2, ignoring the case in which one parameter is scaled up while the other is scaled down. Several other sources of uncertainties related to jet energy scale and resolution, $p_{\text{T}}^{\text{miss}}$ modeling, effects of pileup, and choice of PDF were studied, which collectively have less than

2% impact on our predictions. The uncertainty related to the choice of PDF is evaluated by reweighting the simulation using the variations in the corresponding NNPDF sets (3.0 or 3.1) [60,61]. The statistical treatment of the systematic uncertainties is described in Section 7. Summaries of the dominant systematic uncertainties and their impacts on the yields of the various sources of background and the signal are presented in Table 3.

Among these uncertainties, except for those from the sizes of the CR data and MC samples, the two leading systematic uncertainties that affect the 95% confidence level (CL) upper limits on the signal production cross sections discussed in the next section are the W-tag nonclosure and W-tag correction uncertainties. These degrade the cross section upper limits by up to about 15 and 10%, respectively, depending on the signal model and the SUSY particle masses. The others have much smaller impacts.

7. Results

We perform simultaneous fits using a statistical model of our signal and SM background predictions. The likelihood used for the fits is a product of Poisson distributions, one for each $p_{\text{T}}^{\text{miss}}$ bin of each SR and CR. The systematic uncertainties are included in the likelihood as nuisance parameters with log-normal constraints [122], with the exception of the systematic uncertainties related to the finite size of the simulation, which use the method

described in Ref. [123]. This fitting procedure further constrains the predictions and the uncertainties in the predictions. The yields of the SM backgrounds, determined from the fit applied only to the CRs under the background-only hypothesis, are shown along with the predicted yields of the signals and the observations in Fig. 3. No statistically significant excess of events is observed in the data with respect to the SM background predictions.

We place 95% CL upper limits on the production cross section of either pairs of charginos or a chargino and a neutralino together. The limits are computed based on a binned likelihood fit to the data in all of the b-veto and b-tag SRs and CRs, which takes into account the predicted background and signal yields. A test statistic is used in conjunction with the CL_s criterion [124,125] to set upper limits. The test statistic is the profile likelihood ratio, modified for upper limits [126]. We compute limits using the asymptotic approximation [127].

By comparing the upper limits on the production cross sections to the cross sections predicted for chargino-pair production and for chargino-neutralino production, 95% CL mass exclusion contours are derived. The 95% CL mass exclusion contours within the NLSP-LSP mass plane are shown in Fig. 4 (upper left and upper right) for the TChiWW and TChiWZ models. We exclude NLSP masses between 290 and 670 GeV assuming a pair of charginos are produced and result in a pair of W bosons and a pair of light LSPs. The observed limits are stronger than the expected limits because the observed event yields in the $300 < p_T^{\text{miss}} < 500$ GeV region of the b-veto SR are lower than the SM predictions. For low-mass LSPs, we exclude NLSP masses between 230 and 760 GeV assuming chargino-neutralino production resulting in W and Z bosons and a large p_T^{miss} . For higher NLSP and lower LSP masses, the observed limits are weaker than the expected limits because the observed event yields in the last p_T^{miss} bin of the b-veto SR are higher than the SM predictions. In the case of chargino-neutralino production with a W boson and a Higgs boson, for low-mass LSPs we exclude NLSP masses between 240 and 970 GeV. Fig. 4 (lower) shows limits in the NLSP-LSP mass plane for the TChiWH model. The observed limits are slightly weaker than the expected limits because a few intermediate p_T^{miss} bins of the WH SR contain more observed events than expected.

We also consider models including both $\tilde{\chi}_1^\pm \tilde{\chi}_1^\mp$ and $\tilde{\chi}_1^\pm \tilde{\chi}_2^0$ production where the $\tilde{\chi}_1^\pm$ and $\tilde{\chi}_2^0$ are the mass-degenerate wino-like NLSPs. The expected and observed mass exclusions are presented in Fig. 5 (upper). For the scenarios of $\tilde{\chi}_2^0 \rightarrow Z \tilde{\chi}_1^0$ or $\tilde{\chi}_2^0 \rightarrow H \tilde{\chi}_1^0$, wino-like NLSP masses up to 870 and 960 GeV are excluded, respectively, while exclusions up to 1010 and 1110 GeV are expected under the background-only hypothesis.

Fig. 5 (lower) shows the results for the mass-degenerate higgsino-like NLSP scenario including $\tilde{\chi}_1^\pm \tilde{\chi}_1^\mp$, $\tilde{\chi}_1^\pm \tilde{\chi}_2^0$, $\tilde{\chi}_1^\pm \tilde{\chi}_3^0$, and $\tilde{\chi}_2^0 \tilde{\chi}_3^0$ production. In this scenario, higgsino-like NLSP masses from 300 to 650 GeV are excluded. The expected exclusion reaches from 320 to 810 GeV. The observed exclusion is weaker than expected mainly because of a modest excess in the data over the background prediction in the $300 < p_T^{\text{miss}} < 500$ GeV region of the WH SR.

8. Summary

A search is presented for signatures of electroweak production of charginos and neutralinos in fully hadronic final states. The charginos are assumed to decay to the W boson and the lightest neutralino $\tilde{\chi}_1^0$, and the heavier neutralinos ($\tilde{\chi}_2^0$ and $\tilde{\chi}_3^0$) are assumed to decay to either the Z or Higgs boson (H) and $\tilde{\chi}_1^0$. The decay products of W, Z, or Higgs bosons are clustered into large-radius jets. These jets are categorized based on their mass and a collection of novel jet-tagging algorithms based on deep neural networks. Four search regions, three that require b tags and one that excludes b tags, are constructed to look for chargino-

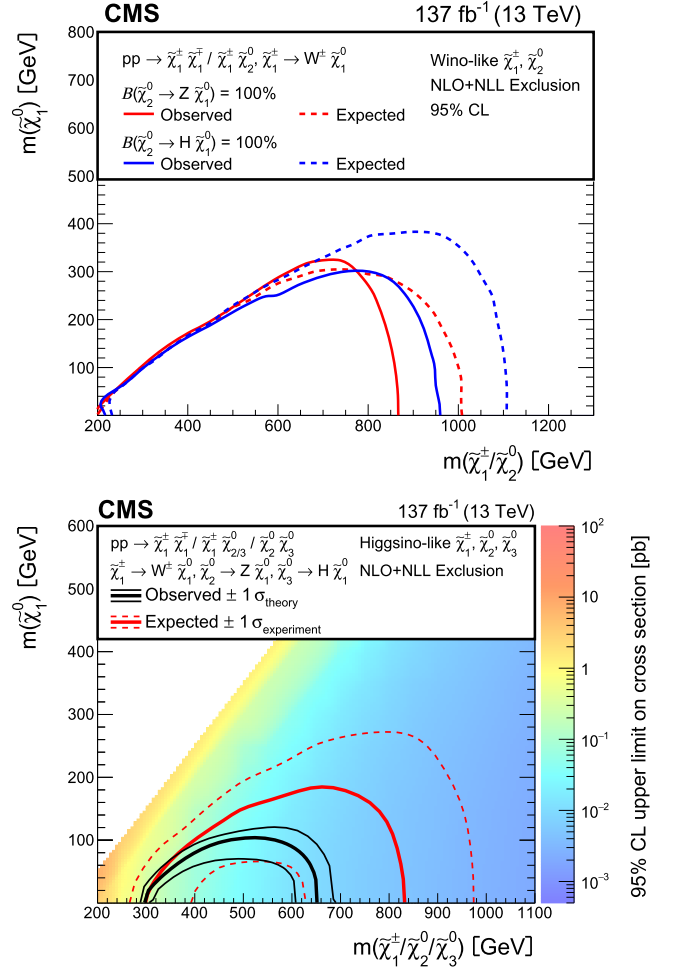


Fig. 5. Expected and observed 95% CL exclusion for mass-degenerate wino-like $\tilde{\chi}_1^\pm \tilde{\chi}_1^\mp$ and $\tilde{\chi}_1^\pm \tilde{\chi}_2^0$ production (upper) and higgsino-like $\tilde{\chi}_1^\pm \tilde{\chi}_1^\mp$, $\tilde{\chi}_1^\pm \tilde{\chi}_2^0$, $\tilde{\chi}_1^\pm \tilde{\chi}_3^0$, and $\tilde{\chi}_2^0 \tilde{\chi}_3^0$ production (lower) as functions of the NLSP and LSP masses. The $\tilde{\chi}_1^\pm$, $\tilde{\chi}_2^0$, and $\tilde{\chi}_3^0$ are considered to be mass degenerate. For the higgsino-like case (lower), the 95% CL upper limits on the production cross sections are also shown, but they are not shown for the wino-like case (upper) because there are two distinct sets of limits depending on the chargino decay mode.

and neutralino-mediated production of a pair of bosons, WW, WZ, or WH, together with a large transverse momentum imbalance. We consider simplified models in which the charginos $\tilde{\chi}_1^\pm$ and the next-to-lightest neutralino $\tilde{\chi}_2^0$ are assumed to be the mass-degenerate next-to-lightest supersymmetric particles (NLSPs). The lightest neutralino $\tilde{\chi}_1^0$ is assumed to be bino-like and to be the lightest supersymmetric particle (LSP). No statistically significant excess of events is observed in the data with respect to the expectation from the standard model.

Using wino-like pair production cross sections, 95% confidence level mass exclusions are derived. For signals with WW, WZ, or WH boson pairs, the NLSP mass exclusion limit for low-mass LSPs extends up to 670, 760, and 970 GeV, respectively. When we consider models including both wino-like NLSP $\tilde{\chi}_1^\pm \tilde{\chi}_2^0$ and $\tilde{\chi}_1^\pm \tilde{\chi}_1^\mp$ production under the assumption that either $\tilde{\chi}_2^0 \rightarrow Z \tilde{\chi}_1^0$ or $\tilde{\chi}_2^0 \rightarrow H \tilde{\chi}_1^0$, the NLSP mass exclusion extends up to 870 and 960 GeV, respectively. Alternatively, with higgsino-like NLSPs $\tilde{\chi}_1^\pm$, $\tilde{\chi}_2^0$, and $\tilde{\chi}_3^0$, the higgsino masses from 300 to 650 GeV are excluded for low-mass LSPs. These mass exclusions significantly improve on those achieved by searches using leptonic probes of SUSY for high NLSP masses.

- [90] J. Alwall, P.C. Schuster, N. Toro, Simplified models for a first characterization of new physics at the LHC, *Phys. Rev. D* 79 (2009) 075020, <https://doi.org/10.1103/PhysRevD.79.075020>, arXiv:0810.3921.
- [91] J. Alwall, M.-P. Le, M. Lisanti, J.G. Wacker, Model-independent jets plus missing energy searches, *Phys. Rev. D* 79 (2009) 015005, <https://doi.org/10.1103/PhysRevD.79.015005>, arXiv:0809.3264.
- [92] D. Alves, et al., Simplified models for LHC new physics searches, *J. Phys. G* 39 (2012) 105005, <https://doi.org/10.1088/0954-3899/39/10/105005>, arXiv:1105.2838.
- [93] CMS Collaboration, Interpretation of searches for supersymmetry with simplified models, *Phys. Rev. D* 88 (2013) 052017, <https://doi.org/10.1103/PhysRevD.88.052017>, arXiv:1301.2175.
- [94] T. Han, S. Padhi, S. Su, Electroweakinos in the light of the Higgs boson, *Phys. Rev. D* 88 (2013) 115010, <https://doi.org/10.1103/PhysRevD.88.115010>, arXiv:1309.5966.
- [95] P. Agrawal, J. Fan, M. Reece, W. Xue, Deciphering the MSSM Higgs mass at future hadron colliders, *J. High Energy Phys.* 06 (2017) 027, [https://doi.org/10.1007/JHEP06\(2017\)027](https://doi.org/10.1007/JHEP06(2017)027), arXiv:1702.05484.
- [96] CMS Collaboration, The CMS experiment at the CERN LHC, *J. Instrum.* 3 (2008) S08004, <https://doi.org/10.1088/1748-0221/3/08/S08004>.
- [97] CMS Collaboration, Particle-flow reconstruction and global event description with the CMS detector, *J. Instrum.* 12 (2017) P10003, <https://doi.org/10.1088/1748-0221/12/10/P10003>, arXiv:1706.04965.
- [98] M. Cacciari, G.P. Salam, G. Soyez, The anti- k_T jet clustering algorithm, *J. High Energy Phys.* 04 (2008) 063, <https://doi.org/10.1088/1126-6708/2008/04/063>, arXiv:0802.1189.
- [99] M. Cacciari, G.P. Salam, G. Soyez, FastJet user manual, *Eur. Phys. J. C* 72 (2012) 1896, <https://doi.org/10.1140/epjc/s10052-012-1896-2>, arXiv:1111.6097.
- [100] CMS Collaboration, Pileup mitigation at CMS in 13 TeV data, *J. Instrum.* 15 (2020) P09018, <https://doi.org/10.1088/1748-0221/15/09/p09018>, arXiv:2003.00503.
- [101] D. Bertolini, P. Harris, M. Low, N. Tran, Pileup per particle identification, *J. High Energy Phys.* 10 (2014) 059, [https://doi.org/10.1007/JHEP10\(2014\)059](https://doi.org/10.1007/JHEP10(2014)059), arXiv:1407.6013.
- [102] CMS Collaboration, Jet energy scale and resolution in the CMS experiment in pp collisions at 8 TeV, *J. Instrum.* 12 (2017) P02014, <https://doi.org/10.1088/1748-0221/12/02/P02014>, arXiv:1607.03663.
- [103] A.J. Larkoski, S. Marzani, G. Soyez, J. Thaler, Soft drop, *J. High Energy Phys.* 05 (2014) 146, [https://doi.org/10.1007/JHEP05\(2014\)146](https://doi.org/10.1007/JHEP05(2014)146), arXiv:1402.2657.
- [104] CMS Collaboration, Performance of missing transverse momentum reconstruction in proton-proton collisions at $\sqrt{s} = 13$ TeV using the CMS detector, *J. Instrum.* 14 (2019) P07004, <https://doi.org/10.1088/1748-0221/14/07/P07004>, arXiv:1903.06078.
- [105] CMS Collaboration, Identification of heavy-flavour jets with the CMS detector in pp collisions at 13 TeV, *J. Instrum.* 13 (2018) P05011, <https://doi.org/10.1088/1748-0221/13/05/P05011>, arXiv:1712.07158.
- [106] CMS Collaboration, Performance of electron reconstruction and selection with the CMS detector in proton-proton collisions at $\sqrt{s} = 8$ TeV, *J. Instrum.* 10 (2015) P06005, <https://doi.org/10.1088/1748-0221/10/06/P06005>, arXiv:1502.02701.
- [107] CMS Collaboration, Performance of the CMS muon detector and muon reconstruction with proton-proton collisions at $\sqrt{s} = 13$ TeV, *J. Instrum.* 13 (2018) P06015, <https://doi.org/10.1088/1748-0221/13/06/P06015>, arXiv:1804.04528.
- [108] CMS Collaboration, Search for supersymmetry in pp collisions at $\sqrt{s} = 13$ TeV in the single-lepton final state using the sum of masses of large-radius jets, *J. High Energy Phys.* 08 (2016) 122, [https://doi.org/10.1007/JHEP08\(2016\)122](https://doi.org/10.1007/JHEP08(2016)122), arXiv:1605.04608.
- [109] CMS Collaboration, Performance of photon reconstruction and identification with the CMS detector in proton-proton collisions at $\sqrt{s} = 8$ TeV, *J. Instrum.* 10 (2015) P08010, <https://doi.org/10.1088/1748-0221/10/08/P08010>, arXiv:1502.02702.
- [110] G. Louppe, M. Kagan, K. Cranmer, Learning to pivot with adversarial networks, *Advances in Neural Information Processing Systems*, vol. 30, 2017, p. 981, arXiv:1611.01046.
- [111] CMS Collaboration, The CMS trigger system, *J. Instrum.* 12 (2017) P01020, <https://doi.org/10.1088/1748-0221/12/01/P01020>, arXiv:1609.02366.
- [112] CMS Collaboration, Description and performance of track and primary-vertex reconstruction with the CMS tracker, *J. Instrum.* 9 (2014) P10009, <https://doi.org/10.1088/1748-0221/9/10/P10009>, arXiv:1405.6569.
- [113] CMS Collaboration, Precision luminosity measurement in proton-proton collisions at $\sqrt{s} = 13$ TeV in 2015 and 2016 at CMS, *Eur. Phys. J. C* 81 (2021) 800, <https://doi.org/10.1140/epjc/s10052-021-09538-2>, arXiv:2104.01927.
- [114] CMS Collaboration, CMS luminosity measurement for the 2017 data-taking period at $\sqrt{s} = 13$ TeV, CMS Physics Analysis Summary, CMS-PAS-LUM-17-004, 2018, <https://cds.cern.ch/record/2621960>.
- [115] CMS Collaboration, CMS luminosity measurement for the 2018 data-taking period at $\sqrt{s} = 13$ TeV, CMS Physics Analysis Summary, CMS-PAS-LUM-18-002, 2019, <https://cds.cern.ch/record/2676164>.
- [116] CMS Collaboration, Measurement of differential $t\bar{t}$ production cross sections in the full kinematic range using lepton+jets events from proton-proton collisions at $\sqrt{s} = 13$ TeV, *Phys. Rev. D* 104 (2021) 092013, <https://doi.org/10.1103/PhysRevD.104.092013>, arXiv:2108.02803.
- [117] ATLAS Collaboration, Measurements of $t\bar{t}$ differential cross-sections of highly boosted top quarks decaying to all-hadronic final states in pp collisions at $\sqrt{s} = 13$ TeV using the ATLAS detector, *Phys. Rev. D* 98 (2018) 012003, <https://doi.org/10.1103/PhysRevD.98.012003>, arXiv:1801.02052.
- [118] CMS Collaboration, Measurement of the production cross section for single top quarks in association with W bosons in proton-proton collisions at $\sqrt{s} = 13$ TeV, *J. High Energy Phys.* 10 (2018) 117, [https://doi.org/10.1007/JHEP10\(2018\)117](https://doi.org/10.1007/JHEP10(2018)117), arXiv:1805.07399.
- [119] CMS Collaboration, Measurements of the pp \rightarrow WZ inclusive and differential production cross section and constraints on charged anomalous triple gauge couplings at $\sqrt{s} = 13$ TeV, *J. High Energy Phys.* 04 (2019) 122, [https://doi.org/10.1007/JHEP04\(2019\)122](https://doi.org/10.1007/JHEP04(2019)122), arXiv:1901.03428.
- [120] CMS Collaboration, Measurements of pp \rightarrow ZZ production cross sections and constraints on anomalous triple gauge couplings at $\sqrt{s} = 13$ TeV, *Eur. Phys. J. C* 81 (2021) 200, <https://doi.org/10.1140/epjc/s10052-020-08817-8>, arXiv:2009.01186.
- [121] CMS Collaboration, W^+W^- boson pair production in proton-proton collisions at $\sqrt{s} = 13$ TeV, *Phys. Rev. D* 102 (2020) 092001, <https://doi.org/10.1103/PhysRevD.102.092001>, arXiv:2009.00119.
- [122] J.S. Conway, Incorporating nuisance parameters in likelihoods for multisource spectra, in: *PHYSTAT 2011*, 2011, p. 115, arXiv:1103.0354.
- [123] R. Barlow, C. Beeston, Fitting using finite Monte Carlo samples, *Comput. Phys. Commun.* 77 (1993) 219, [https://doi.org/10.1016/0010-4655\(93\)90005-W](https://doi.org/10.1016/0010-4655(93)90005-W).
- [124] A.L. Read, Presentation of search results: the CL_s technique, *J. Phys. G* 28 (2002) 2693, <https://doi.org/10.1088/0954-3899/28/10/313>.
- [125] T. Junk, Confidence level computation for combining searches with small statistics, *Nucl. Instrum. Methods A* 434 (1999) 435, [https://doi.org/10.1016/S0168-9002\(99\)00498-2](https://doi.org/10.1016/S0168-9002(99)00498-2), arXiv:hep-ex/9902006.
- [126] ATLAS Collaboration, CMS Collaboration, LHC Higgs Combination Group, Procedure for the LHC Higgs boson search combination in Summer 2011, Technical Report CMS-NOTE-2011-005, ATL-PHYS-PUB-2011-11, 2011, <https://cds.cern.ch/record/1379837>.
- [127] G. Cowan, K. Cranmer, E. Gross, O. Vitells, Asymptotic formulae for likelihood-based tests of new physics, *Eur. Phys. J. C* 71 (2011) 1554, <https://doi.org/10.1140/epjc/s10052-011-1554-0>, arXiv:1007.1727; Erratum: <https://doi.org/10.1140/epjc/s10052-013-2501-z>.

The CMS Collaboration

A. Tumasyan¹

Yerevan Physics Institute, Yerevan, Armenia

W. Adam, J.W. Andrejkovic, T. Bergauer, S. Chatterjee, K. Damanakis, M. Dragicevic, A. Escalante Del Valle, R. Frühwirth², M. Jeitler², N. Krammer, L. Lechner, D. Liko, I. Mikulec, P. Paulitsch, F.M. Pitters, J. Schieck², R. Schöfbeck, D. Schwarz, S. Templ, W. Waltenberger, C.-E. Wulz²

Institut für Hochenergiephysik, Vienna, Austria

M.R. Darwish³, E.A. De Wolf, T. Janssen, T. Kello⁴, A. Lelek, H. Rejeb Sfar, P. Van Mechelen, S. Van Putte, N. Van Remortel

Universiteit Antwerpen, Antwerpen, Belgium

E.S. Bols, J. D'Hondt, M. Delcourt, H. El Faham, S. Lowette, S. Moortgat, A. Morton, D. Müller, A.R. Sahasransu, S. Tavernier, W. Van Doninck, D. Vannerom

Vrije Universiteit Brussel, Brussel, Belgium

D. Beghin, B. Bilin, B. Clerbaux, G. De Lentdecker, L. Favart, A.K. Kalsi, K. Lee, M. Mahdavihorrami, I. Makarenko, L. Moureaux, S. Paredes, L. Pétré, A. Popov, N. Postiau, E. Starling, L. Thomas, M. Vanden Bemden, C. Vander Velde, P. Vanlaer

Université Libre de Bruxelles, Bruxelles, Belgium

T. Cornelis, D. Dobur, J. Knolle, L. Lambrecht, G. Mestdach, M. Niedziela, C. Rendón, C. Roskas, A. Samalan, K. Skovpen, M. Tytgat, B. Vermassen, L. Wezenbeek

Ghent University, Ghent, Belgium

A. Benecke, A. Bethani, G. Bruno, F. Bury, C. Caputo, P. David, C. Delaere, I.S. Donertas, A. Giammanco, K. Jaffel, Sa. Jain, V. Lemaître, K. Mondal, J. Prisciandaro, A. Taliercio, M. Teklishyn, T.T. Tran, P. Vischia, S. Wertz

Université Catholique de Louvain, Louvain-la-Neuve, Belgium

G.A. Alves, C. Hensel, A. Moraes, P. Rebello Teles

Centro Brasileiro de Pesquisas Físicas, Rio de Janeiro, Brazil

W.L. Aldá Júnior, M. Alves Gallo Pereira, M. Barroso Ferreira Filho, H. Brandao Malbouisson, W. Carvalho, J. Chinellato⁵, E.M. Da Costa, G.G. Da Silveira⁶, D. De Jesus Damiao, V. Dos Santos Sousa, S. Fonseca De Souza, C. Mora Herrera, K. Mota Amarilo, L. Mundim, H. Nogima, A. Santoro, S.M. Silva Do Amaral, A. Sznajder, M. Thiel, F. Torres Da Silva De Araujo⁷, A. Vilela Pereira

Universidade do Estado do Rio de Janeiro, Rio de Janeiro, Brazil

C.A. Bernardes⁶, L. Calligaris, T.R. Fernandez Perez Tomei, E.M. Gregores, D.S. Lemos, P.G. Mercadante, S.F. Novaes, Sandra S. Padula

Universidade Estadual Paulista, Universidade Federal do ABC, São Paulo, Brazil

A. Aleksandrov, G. Antchev, R. Hadjiiska, P. Iaydjiev, M. Misheva, M. Rodozov, M. Shopova, G. Sultanov

Institute for Nuclear Research and Nuclear Energy, Bulgarian Academy of Sciences, Sofia, Bulgaria

A. Dimitrov, T. Ivanov, L. Litov, B. Pavlov, P. Petkov, A. Petrov

University of Sofia, Sofia, Bulgaria

T. Cheng, T. Javaid⁸, M. Mittal, L. Yuan

Beihang University, Beijing, China

M. Ahmad, G. Bauer, C. Dozen, Z. Hu, J. Martins⁹, Y. Wang, K. Yi^{10,11}

Department of Physics, Tsinghua University, Beijing, China

E. Chapon, G.M. Chen⁸, H.S. Chen⁸, M. Chen, F. Iemmi, A. Kapoor, D. Leggat, H. Liao, Z.-A. Liu¹², V. Milosevic, F. Monti, R. Sharma, J. Tao, J. Thomas-Wilsker, J. Wang, H. Zhang, J. Zhao

Institute of High Energy Physics, Beijing, China

A. Agapitos, Y. An, Y. Ban, C. Chen, A. Levin, Q. Li, X. Lyu, Y. Mao, S.J. Qian, D. Wang, J. Xiao, H. Yang

State Key Laboratory of Nuclear Physics and Technology, Peking University, Beijing, China

M. Lu, Z. You

Sun Yat-Sen University, Guangzhou, China

X. Gao⁴, H. Okawa, Y. Zhang

Institute of Modern Physics and Key Laboratory of Nuclear Physics and Ion-beam Application (MOE) – Fudan University, Shanghai, China

Z. Lin, M. Xiao

Zhejiang University, Hangzhou, Zhejiang, China

C. Avila, A. Cabrera, C. Florez, J. Fraga

Universidad de Los Andes, Bogota, Colombia

J. Mejia Guisao, F. Ramirez, J.D. Ruiz Alvarez

Universidad de Antioquia, Medellin, Colombia

D. Giljanovic, N. Godinovic, D. Lelas, I. Puljak

University of Split, Faculty of Electrical Engineering, Mechanical Engineering and Naval Architecture, Split, Croatia

Z. Antunovic, M. Kovac, T. Sculac

University of Split, Faculty of Science, Split, Croatia

V. Brigljevic, D. Ferencek, D. Majumder, M. Roguljic, A. Starodumov¹³, T. Susa

Institute Rudjer Boskovic, Zagreb, Croatia

A. Attikis, K. Christoforou, A. Ioannou, G. Kole, M. Kolosova, S. Konstantinou, J. Mousa, C. Nicolaou, F. Ptochos, P.A. Razis, H. Rykaczewski, H. Saka

University of Cyprus, Nicosia, Cyprus

M. Finger¹³, M. Finger Jr.¹³, A. Kveton

Charles University, Prague, Czech Republic

E. Ayala

Escuela Politecnica Nacional, Quito, Ecuador

E. Carrera Jarrin

Universidad San Francisco de Quito, Quito, Ecuador

H. Abdalla¹⁴, S. Khalil¹⁵

Academy of Scientific Research and Technology of the Arab Republic of Egypt, Egyptian Network of High Energy Physics, Cairo, Egypt

A. Lotfy, M.A. Mahmoud

Center for High Energy Physics (CHEP-FU), Fayoum University, El-Fayoum, Egypt

S. Bhowmik, R.K. Dewanjee, K. Ehataht, M. Kadastik, S. Nandan, C. Nielsen, J. Pata, M. Raidal, L. Tani, C. Veelken

National Institute of Chemical Physics and Biophysics, Tallinn, Estonia

P. Eerola, H. Kirschenmann, K. Osterberg, M. Voutilainen

Department of Physics, University of Helsinki, Helsinki, Finland

S. Bharthuar, E. Brücken, F. Garcia, J. Havukainen, M.S. Kim, R. Kinnunen, T. Lampén, K. Lassila-Perini, S. Lehti, T. Lindén, M. Lotti, L. Martikainen, M. Myllymäki, J. Ott, H. Siikonen, E. Tuominen, J. Tuominiemi

Helsinki Institute of Physics, Helsinki, Finland

P. Luukka, H. Petrow, T. Tuuva

Lappeenranta-Lahti University of Technology, Lappeenranta, Finland

C. Amendola, M. Besancon, F. Couderc, M. Dejardin, D. Denegri, J.L. Faure, F. Ferri, S. Ganjour, P. Gras, G. Hamel de Monchenault, P. Jarry, B. Lenzi, E. Locci, J. Malcles, J. Rander, A. Rosowsky, M.Ö. Sahin, A. Savoy-Navarro¹⁶, M. Titov, G.B. Yu

IRFU, CEA, Université Paris-Saclay, Gif-sur-Yvette, France

S. Ahuja, F. Beaudette, M. Bonanomi, A. Buchot Perraguin, P. Busson, A. Cappati, C. Charlot, O. Davignon, B. Diab, G. Falmagne, S. Ghosh, R. Granier de Cassagnac, A. Hakimi, I. Kucher, J. Motta, M. Nguyen, C. Ochando, P. Paganini, J. Rembser, R. Salerno, U. Sarkar, J.B. Sauvan, Y. Sirois, A. Tarabini, A. Zabi, A. Zghiche

Laboratoire Leprince-Ringuet, CNRS/IN2P3, Ecole Polytechnique, Institut Polytechnique de Paris, Palaiseau, France

J.-L. Agram¹⁷, J. Andrea, D. Apparú, D. Bloch, G. Bourgatte, J.-M. Brom, E.C. Chabert, C. Collard, D. Darej, J.-C. Fontaine¹⁷, U. Goerlach, C. Grimault, A.-C. Le Bihan, E. Nibigira, P. Van Hove

Université de Strasbourg, CNRS, IPHC UMR 7178, Strasbourg, France

E. Asilar, S. Beauceron, C. Bernet, G. Boudoul, C. Camen, A. Carle, N. Chanon, D. Contardo, P. Depasse, H. El Mamouni, J. Fay, S. Gascon, M. Gouzevitch, B. Ille, I.B. Laktineh, H. Lattaud, A. Lesauvage, M. Lethuillier, L. Mirabito, S. Perries, K. Shchablo, V. Sordini, L. Torterotot, G. Touquet, M. Vander Donckt, S. Viret

Institut de Physique des 2 Infinis de Lyon (IP2I), Villeurbanne, France

I. Lomidze, T. Toriashvili¹⁸, Z. Tsamalaidze¹³

Georgian Technical University, Tbilisi, Georgia

V. Botta, L. Feld, K. Klein, M. Lipinski, D. Meuser, A. Pauls, N. Röwert, J. Schulz, M. Teroerde

RWTH Aachen University, I. Physikalisches Institut, Aachen, Germany

A. Dodonova, D. Eliseev, M. Erdmann, P. Fackeldey, B. Fischer, T. Hebbeker, K. Hoepfner, F. Ivone, L. Mastrolorenzo, M. Merschmeyer, A. Meyer, G. Mocellin, S. Mondal, S. Mukherjee, D. Noll, A. Novak, A. Pozdnyakov, Y. Rath, H. Reithler, A. Schmidt, S.C. Schuler, A. Sharma, L. Vigilante, S. Wiedenbeck, S. Zaleski

RWTH Aachen University, III. Physikalisches Institut A, Aachen, Germany

C. Dziwok, G. Flügge, W. Haj Ahmad¹⁹, O. Hlushchenko, T. Kress, A. Nowack, O. Pooth, D. Roy, A. Stahl²⁰, T. Ziemons, A. Zolt

RWTH Aachen University, III. Physikalisches Institut B, Aachen, Germany

H. Aarup Petersen, M. Aldaya Martin, P. Asmuss, S. Baxter, M. Bayatmakou, O. Behnke, A. Bermúdez Martínez, S. Bhattacharya, A.A. Bin Anuar, F. Blekman, K. Borras²¹, D. Brunner, A. Campbell, A. Cardini, C. Cheng, F. Colombina, S. Consuegra Rodríguez, G. Correia Silva, V. Danilov, M. De Silva, L. Didukh, G. Eckerlin, D. Eckstein, L.I. Estevez Banos, O. Filatov, E. Gallo²², A. Geiser, A. Giraldi, A. Grohsjean, M. Guthoff, A. Jafari²³, N.Z. Jomhari, A. Kasem²¹, M. Kasemann, H. Kaveh, C. Kleinwort, R. Kogler, D. Krücker, W. Lange, K. Lipka, W. Lohmann²⁴, R. Mankel, I.-A. Melzer-Pellmann, M. Mendizabal Morentin, J. Metwally, A.B. Meyer, M. Meyer, J. Mnich, A. Mussgiller, A. Nürnberg, Y. Otariid, D. Pérez Adán, D. Pitzl, A. Raspereza, B. Ribeiro Lopes, J. Rübenach, A. Saggio, A. Saibel,

M. Savitskyi, M. Scham²⁵, V. Scheurer, S. Schnake, P. Schütze, C. Schwanenberger²², M. Shchedrolosiev, R.E. Sosa Ricardo, D. Stafford, N. Tonon, M. Van De Klundert, F. Vazzoler, R. Walsh, D. Walter, Q. Wang, Y. Wen, K. Wichmann, L. Wiens, C. Wissing, S. Wuchterl

Deutsches Elektronen-Synchrotron, Hamburg, Germany

R. Aggleton, S. Albrecht, S. Bein, L. Benato, P. Connor, K. De Leo, M. Eich, F. Feindt, A. Fröhlich, C. Garbers, E. Garutti, P. Gunnellini, M. Hajheidari, J. Haller, A. Hinzmann, G. Kasieczka, R. Klanner, T. Kramer, V. Kutzner, J. Lange, T. Lange, A. Lobanov, A. Malara, A. Mehta, A. Nigamova, K.J. Pena Rodriguez, M. Rieger, O. Rieger, P. Schleper, M. Schröder, J. Schwandt, J. Sonneveld, H. Stadie, G. Steinbrück, A. Tews, I. Zoi

University of Hamburg, Hamburg, Germany

J. Bechtel, S. Brommer, M. Burkart, E. Butz, R. Caspart, T. Chwalek, W. De Boer[†], A. Dierlamm, A. Droll, K. El Morabit, N. Faltermann, M. Giffels, J.O. Gosewisch, A. Gottmann, F. Hartmann²⁰, C. Heidecker, U. Husemann, P. Keicher, R. Koppenhöfer, S. Maier, M. Metzler, S. Mitra, Th. Müller, M. Neukum, G. Quast, K. Rabbertz, J. Rauser, D. Savoie, M. Schnepf, D. Seith, I. Shvetsov, H.J. Simonis, R. Ulrich, J. Van Der Linden, R.F. Von Cube, M. Wassmer, M. Weber, S. Wieland, R. Wolf, S. Wozniewski, S. Wunsch

Karlsruher Institut fuer Technologie, Karlsruhe, Germany

G. Anagnostou, G. Daskalakis, A. Kyriakis, A. Stakia

Institute of Nuclear and Particle Physics (INPP), NCSR Demokritos, Aghia Paraskevi, Greece

M. Diamantopoulou, D. Karasavvas, P. Kontaxakis, C.K. Koraka, A. Manousakis-Katsikakis, A. Panagiotou, I. Papavergou, N. Saoulidou, K. Theofilatos, E. Tziaferi, K. Vellidis, E. Vourliotis

National and Kapodistrian University of Athens, Athens, Greece

G. Bakas, K. Kousouris, I. Papakrivopoulos, G. Tsipolitis, A. Zacharopoulou

National Technical University of Athens, Athens, Greece

K. Adamidis, I. Bestintzanos, I. Evangelou, C. Foudas, P. Gianneios, P. Katsoulis, P. Kokkas, N. Manthos, I. Papadopoulos, J. Strologas

University of Ioánnina, Ioánnina, Greece

M. Csanád, K. Farkas, M.M.A. Gadallah²⁶, S. Lökös²⁷, P. Major, K. Mandal, G. Pásztor, A.J. Rádl, O. Surányi, G.I. Veres

MTA-ELTE Lendület CMS Particle and Nuclear Physics Group, Eötvös Loránd University, Budapest, Hungary

M. Bartók²⁸, G. Bencze, C. Hajdu, D. Horvath^{29,30}, F. Sikler, V. Veszpremi

Wigner Research Centre for Physics, Budapest, Hungary

S. Czellar, D. Fasanella, F. Fienga, J. Karancsi²⁸, J. Molnar, Z. Szillasi, D. Teyssier

Institute of Nuclear Research ATOMKI, Debrecen, Hungary

P. Raics, Z.L. Trocsanyi³¹, B. Ujvari

Institute of Physics, University of Debrecen, Debrecen, Hungary

T. Csorgo³², F. Nemes³², T. Novak

Karoly Robert Campus, MATE Institute of Technology, Gyongyos, Hungary

S. Bansal, S.B. Beri, V. Bhatnagar, G. Chaudhary, S. Chauhan, N. Dhingra³³, R. Gupta, A. Kaur, H. Kaur, M. Kaur, P. Kumari, M. Meena, K. Sandeep, J.B. Singh, A.K. Viridi

Panjab University, Chandigarh, India

A. Ahmed, A. Bhardwaj, B.C. Choudhary, M. Gola, S. Keshri, A. Kumar, M. Naimuddin, P. Priyanka, K. Ranjan, A. Shah

University of Delhi, Delhi, India

M. Bharti³⁴, R. Bhattacharya, S. Bhattacharya, D. Bhowmik, S. Dutta, S. Dutta, B. Gomber³⁵, M. Maity³⁶, P. Palit, P.K. Rout, G. Saha, B. Sahu, S. Sarkar, M. Sharan

Saha Institute of Nuclear Physics, HBNI, Kolkata, India

P.K. Behera, S.C. Behera, P. Kalbhor, J.R. Komaragiri³⁷, D. Kumar³⁷, A. Muhammad, L. Panwar³⁷, R. Pradhan, P.R. Pujahari, A. Sharma, A.K. Sikdar, P.C. Tiwari³⁷

Indian Institute of Technology Madras, Madras, India

K. Naskar³⁸

Bhabha Atomic Research Centre, Mumbai, India

T. Aziz, S. Dugad, M. Kumar, G.B. Mohanty

Tata Institute of Fundamental Research-A, Mumbai, India

S. Banerjee, R. Chudasama, M. Guchait, S. Karmakar, S. Kumar, G. Majumder, K. Mazumdar, S. Mukherjee

Tata Institute of Fundamental Research-B, Mumbai, India

S. Bahinipati³⁹, C. Kar, P. Mal, T. Mishra, V.K. Muraleedharan Nair Bindhu⁴⁰, A. Nayak⁴⁰, P. Saha, N. Sur, S.K. Swain, D. Vats⁴⁰

National Institute of Science Education and Research, An OCC of Homi Bhabha National Institute, Bhubaneswar, Odisha, India

A. Alpana, S. Dube, B. Kansal, A. Laha, S. Pandey, A. Rastogi, S. Sharma

Indian Institute of Science Education and Research (IISER), Pune, India

H. Bakhshiansohi⁴¹, E. Khazaie, M. Zeinali⁴²

Isfahan University of Technology, Isfahan, Iran

S. Chenarani⁴³, S.M. Etesami, M. Khakzad, M. Mohammadi Najafabadi

Institute for Research in Fundamental Sciences (IPM), Tehran, Iran

M. Grunewald

University College Dublin, Dublin, Ireland

M. Abbrescia^{a,b}, R. Aly^{a,c,44}, C. Aruta^{a,b}, A. Colaleo^a, D. Creanza^{a,c}, N. De Filippis^{a,c}, M. De Palma^{a,b}, A. Di Florio^{a,b}, A. Di Pilato^{a,b}, W. Elmetenawee^{a,b}, F. Errico^{a,b}, L. Fiore^a, A. Gelmi^{a,b}, M. Gul^a, G. Iaselli^{a,c}, M. Ince^{a,b}, S. Lezki^{a,b}, G. Maggi^{a,c}, M. Maggi^a, I. Margjeka^{a,b}, V. Mastrapasqua^{a,b}, S. My^{a,b}, S. Nuzzo^{a,b}, A. Pellecchia^{a,b}, A. Pompili^{a,b}, G. Pugliese^{a,c}, D. Ramos^a, A. Ranieri^a, G. Selvaggi^{a,b}, L. Silvestris^a, F.M. Simone^{a,b}, Ü. Sözbilir^a, R. Venditti^a, P. Verwilligen^a

^a INFN Sezione di Bari, Bari, Italy

^b Università di Bari, Bari, Italy

^c Politecnico di Bari, Bari, Italy

G. Abbiendi^a, C. Battilana^{a,b}, D. Bonacorsi^{a,b}, L. Borghonovi^a, L. Brigliadori^a, R. Campanini^{a,b}, P. Capiluppi^{a,b}, A. Castro^{a,b}, F.R. Cavallo^a, C. Ciocca^a, M. Cuffiani^{a,b}, G.M. Dallavalle^a, T. Diotallevi^{a,b}, F. Fabbri^a, A. Fanfani^{a,b}, P. Giacomelli^a, L. Giommi^{a,b}, C. Grandi^a, L. Guiducci^{a,b}, S. Lo Meo^{a,45}, L. Lunerti^{a,b}, S. Marcellini^a, G. Masetti^a, F.L. Navarria^{a,b}, A. Perrotta^a, F. Primavera^{a,b}, A.M. Rossi^{a,b}, T. Rovelli^{a,b}, G.P. Siroli^{a,b}

^a INFN Sezione di Bologna, Bologna, Italy

^b Università di Bologna, Bologna, Italy

S. Albergo ^{a,b,46}, S. Costa ^{a,b,46}, A. Di Mattia ^a, R. Potenza ^{a,b}, A. Tricomi ^{a,b,46}, C. Tuve ^{a,b}

^a INFN Sezione di Catania, Catania, Italy

^b Università di Catania, Catania, Italy

G. Barbagli ^a, A. Cassese ^a, R. Ceccarelli ^{a,b}, V. Ciulli ^{a,b}, C. Civinini ^a, R. D'Alessandro ^{a,b}, E. Focardi ^{a,b}, G. Latino ^{a,b}, P. Lenzi ^{a,b}, M. Lizzo ^{a,b}, M. Meschini ^a, S. Paoletti ^a, R. Seidita ^{a,b}, G. Sguazzoni ^a, L. Viliani ^a

^a INFN Sezione di Firenze, Firenze, Italy

^b Università di Firenze, Firenze, Italy

L. Benussi, S. Bianco, D. Piccolo

INFN Laboratori Nazionali di Frascati, Frascati, Italy

M. Bozzo ^{a,b}, F. Ferro ^a, R. Mulargia ^a, E. Robutti ^a, S. Tosi ^{a,b}

^a INFN Sezione di Genova, Genova, Italy

^b Università di Genova, Genova, Italy

A. Benaglia ^a, G. Boldrini ^a, F. Brivio ^{a,b}, F. Cetorelli ^{a,b}, F. De Guio ^{a,b}, M.E. Dinardo ^{a,b}, P. Dini ^a, S. Gennai ^a, A. Ghezzi ^{a,b}, P. Govoni ^{a,b}, L. Guzzi ^{a,b}, M.T. Lucchini ^{a,b}, M. Malberti ^a, S. Malvezzi ^a, A. Massironi ^a, D. Menasce ^a, L. Moroni ^a, M. Paganoni ^{a,b}, D. Pedrini ^a, B.S. Pinolini ^a, S. Ragazzi ^{a,b}, N. Redaelli ^a, T. Tabarelli de Fatis ^{a,b}, D. Valsecchi ^{a,b,20}, D. Zuolo ^{a,b}

^a INFN Sezione di Milano-Bicocca, Milano, Italy

^b Università di Milano-Bicocca, Milano, Italy

S. Buontempo ^a, F. Carnevali ^{a,b}, N. Cavallo ^{a,c}, A. De Iorio ^{a,b}, F. Fabozzi ^{a,c}, A.O.M. Iorio ^{a,b}, L. Lista ^{a,b,47}, S. Meola ^{a,d,20}, P. Paolucci ^{a,20}, B. Rossi ^a, C. Sciacca ^{a,b}

^a INFN Sezione di Napoli, Napoli, Italy

^b Università di Napoli 'Federico II', Napoli, Italy

^c Università della Basilicata, Potenza, Italy

^d Università G. Marconi, Roma, Italy

P. Azzi ^a, N. Bacchetta ^a, D. Bisello ^{a,b}, P. Bortignon ^a, A. Bragagnolo ^{a,b}, R. Carlin ^{a,b}, P. Checchia ^a, T. Dorigo ^a, U. Dosselli ^a, F. Gasparini ^{a,b}, U. Gasparini ^{a,b}, G. Grosso ^a, L. Layer ^{a,48}, E. Lusiani ^a, M. Margoni ^{a,b}, A.T. Meneguzzo ^{a,b}, J. Pazzini ^{a,b}, P. Ronchese ^{a,b}, R. Rossin ^{a,b}, F. Simonetto ^{a,b}, G. Strong ^a, M. Tosi ^{a,b}, H. Yarar ^{a,b}, M. Zanetti ^{a,b}, P. Zotto ^{a,b}, A. Zucchetta ^{a,b}, G. Zumerle ^{a,b}

^a INFN Sezione di Padova, Padova, Italy

^b Università di Padova, Padova, Italy

^c Università di Trento, Trento, Italy

C. Aimè ^{a,b}, A. Braghieri ^a, S. Calzaferri ^{a,b}, D. Fiorina ^{a,b}, P. Montagna ^{a,b}, S.P. Ratti ^{a,b}, V. Re ^a, C. Riccardi ^{a,b}, P. Salvini ^a, I. Vai ^a, P. Vitulo ^{a,b}

^a INFN Sezione di Pavia, Pavia, Italy

^b Università di Pavia, Pavia, Italy

P. Asenov ^{a,49}, G.M. Bilei ^a, D. Ciangottini ^{a,b}, L. Fanò ^{a,b}, M. Magherini ^{a,b}, G. Mantovani ^{a,b}, V. Mariani ^{a,b}, M. Menichelli ^a, F. Moscatelli ^{a,49}, A. Piccinelli ^{a,b}, M. Presilla ^{a,b}, A. Rossi ^{a,b}, A. Santocchia ^{a,b}, D. Spiga ^a, T. Tedeschi ^{a,b}

^a INFN Sezione di Perugia, Perugia, Italy

^b Università di Perugia, Perugia, Italy

P. Azzurri ^a, G. Bagliesi ^a, V. Bertacchi ^{a,c}, L. Bianchini ^a, T. Boccali ^a, E. Bossini ^{a,b}, R. Castaldi ^a, M.A. Ciocci ^{a,b}, V. D'Amante ^{a,d}, R. Dell'Orso ^a, M.R. Di Domenico ^{a,d}, S. Donato ^a, A. Giassi ^a, F. Ligabue ^{a,c}, E. Manca ^{a,c}, G. Mandorli ^{a,c}, D. Matos Figueiredo ^a, A. Messineo ^{a,b}, M. Musich ^a, F. Palla ^a, S. Parolia ^{a,b}, G. Ramirez-Sanchez ^{a,c}, A. Rizzi ^{a,b}, G. Rolandi ^{a,c}, S. Roy Chowdhury ^{a,c}, A. Scribano ^a, N. Shafiei ^{a,b}, P. Spagnolo ^a, R. Tenchini ^a, G. Tonelli ^{a,b}, N. Turini ^{a,d}, A. Venturi ^a, P.G. Verdini ^a

^a INFN Sezione di Pisa, Pisa, Italy

^b Università di Pisa, Pisa, Italy

^c Scuola Normale Superiore di Pisa, Pisa, Italy^d Università di Siena, Siena, Italy

P. Barria^a, M. Campana^{a,b}, F. Cavallari^a, D. Del Re^{a,b}, E. Di Marco^a, M. Diemoz^a, E. Longo^{a,b},
 P. Meridiani^a, G. Organtini^{a,b}, F. Pandolfi^a, R. Paramatti^{a,b}, C. Quaranta^{a,b}, S. Rahatlou^{a,b}, C. Rovelli^a,
 F. Santanastasio^{a,b}, L. Soffi^a, R. Tramontano^{a,b}

^a INFN Sezione di Roma, Roma, Italy^b Sapienza Università di Roma, Roma, Italy

N. Amapane^{a,b}, R. Arcidiacono^{a,c}, S. Argiro^{a,b}, M. Arneodo^{a,c}, N. Bartosik^a, R. Bellan^{a,b}, A. Bellora^{a,b},
 J. Berenguer Antequera^{a,b}, C. Biino^a, N. Cartiglia^a, M. Costa^{a,b}, R. Covarelli^{a,b}, N. Demaria^a, B. Kiani^{a,b},
 F. Legger^a, C. Mariotti^a, S. Maselli^a, E. Migliore^{a,b}, E. Monteil^{a,b}, M. Monteno^a, M.M. Obertino^{a,b},
 G. Ortona^a, L. Pacher^{a,b}, N. Pastrone^a, M. Pelliccioni^a, M. Ruspa^{a,c}, K. Shchelina^a, F. Siviero^{a,b}, V. Sola^a,
 A. Solano^{a,b}, D. Soldi^{a,b}, A. Staiano^a, M. Tornago^{a,b}, D. Trocino^a, A. Vagnerini^{a,b}

^a INFN Sezione di Torino, Torino, Italy^b Università di Torino, Torino, Italy^c Università del Piemonte Orientale, Novara, Italy

S. Belforte^a, V. Candelise^{a,b}, M. Casarsa^a, F. Cossutti^a, A. Da Rold^{a,b}, G. Della Ricca^{a,b}, G. Sorrentino^{a,b}

^a INFN Sezione di Trieste, Trieste, Italy^b Università di Trieste, Trieste, Italy

S. Dogra, C. Huh, B. Kim, D.H. Kim, G.N. Kim, J. Kim, J. Lee, S.W. Lee, C.S. Moon, Y.D. Oh, S.I. Pak,
 S. Sekmen, Y.C. Yang

Kyungpook National University, Daegu, Korea

H. Kim, D.H. Moon

Chonnam National University, Institute for Universe and Elementary Particles, Kwangju, Korea

B. Francois, T.J. Kim, J. Park

Hanyang University, Seoul, Korea

S. Cho, S. Choi, B. Hong, K. Lee, K.S. Lee, J. Lim, J. Park, S.K. Park, J. Yoo

Korea University, Seoul, Korea

J. Goh, A. Gurtu

Kyung Hee University, Department of Physics, Seoul, Korea

H.S. Kim, Y. Kim

Sejong University, Seoul, Korea

J. Almond, J.H. Bhyun, J. Choi, S. Jeon, J. Kim, J.S. Kim, S. Ko, H. Kwon, H. Lee, S. Lee, B.H. Oh, M. Oh,
 S.B. Oh, H. Seo, U.K. Yang, I. Yoon

Seoul National University, Seoul, Korea

W. Jang, D.Y. Kang, Y. Kang, S. Kim, B. Ko, J.S.H. Lee, Y. Lee, J.A. Merlin, I.C. Park, Y. Roh, M.S. Ryu,
 D. Song, I.J. Watson, S. Yang

University of Seoul, Seoul, Korea

S. Ha, H.D. Yoo

Yonsei University, Department of Physics, Seoul, Korea

M. Choi, H. Lee, Y. Lee, I. Yu

Sungkyunkwan University, Suwon, Korea

T. Beyrouthy, Y. Maghrbi

College of Engineering and Technology, American University of the Middle East (AUM), Dasman, Kuwait

K. Dreimanis, V. Veckalns

Riga Technical University, Riga, Latvia

M. Ambrozas, A. Carvalho Antunes De Oliveira, A. Juodagalvis, A. Rinkevicius, G. Tamulaitis

Vilnius University, Vilnius, Lithuania

N. Bin Norjoharuddeen, Z. Zolkapli

National Centre for Particle Physics, Universiti Malaya, Kuala Lumpur, Malaysia

J.F. Benitez, A. Castaneda Hernandez, H.A. Encinas Acosta, L.G. Gallegos Maríñez, M. León Coello, J.A. Murillo Quijada, A. Sehrawat, L. Valencia Palomo

Universidad de Sonora (UNISON), Hermosillo, Mexico

G. Ayala, H. Castilla-Valdez, E. De La Cruz-Burelo, I. Heredia-De La Cruz⁵⁰, R. Lopez-Fernandez, C.A. Mondragon Herrera, D.A. Perez Navarro, R. Reyes-Almanza, A. Sánchez Hernández

Centro de Investigación y de Estudios Avanzados del IPN, Mexico City, Mexico

S. Carrillo Moreno, C. Oropeza Barrera, F. Vazquez Valencia

Universidad Iberoamericana, Mexico City, Mexico

I. Pedraza, H.A. Salazar Ibarguen, C. Uribe Estrada

Benemerita Universidad Autonoma de Puebla, Puebla, Mexico

J. Mijuskovic⁵¹, N. Raicevic

University of Montenegro, Podgorica, Montenegro

D. Krofcheck

University of Auckland, Auckland, New Zealand

P.H. Butler

University of Canterbury, Christchurch, New Zealand

A. Ahmad, M.I. Asghar, A. Awais, M.I.M. Awan, H.R. Hoorani, W.A. Khan, M.A. Shah, M. Shoaib, M. Waqas

National Centre for Physics, Quaid-I-Azam University, Islamabad, Pakistan

V. Avati, L. Grzanka, M. Malawski

AGH University of Science and Technology Faculty of Computer Science, Electronics and Telecommunications, Krakow, Poland

H. Bialkowska, M. Bluj, B. Boimska, M. Górski, M. Kazana, M. Szleper, P. Zalewski

National Centre for Nuclear Research, Swierk, Poland

K. Bunkowski, K. Doroba, A. Kalinowski, M. Konecki, J. Krolikowski

Institute of Experimental Physics, Faculty of Physics, University of Warsaw, Warsaw, Poland

M. Araujo, P. Bargassa, D. Bastos, A. Boletti, P. Faccioli, M. Gallinaro, J. Hollar, N. Leonardo, T. Niknejad, M. Pisano, J. Seixas, O. Toldaiev, J. Varela

Laboratório de Instrumentação e Física Experimental de Partículas, Lisboa, Portugal

P. Adzic⁵², M. Dordevic, P. Milenovic, J. Milosevic

VINCA Institute of Nuclear Sciences, University of Belgrade, Belgrade, Serbia

M. Aguilar-Benitez, J. Alcaraz Maestre, A. Álvarez Fernández, I. Bachiller, M. Barrio Luna, Cristina F. Bedoya, C.A. Carrillo Montoya, M. Cepeda, M. Cerrada, N. Colino, B. De La Cruz, A. Delgado Peris, J.P. Fernández Ramos, J. Flix, M.C. Fouz, O. Gonzalez Lopez, S. Goy Lopez, J.M. Hernandez, M.I. Josa, J. León Holgado, D. Moran, Á. Navarro Tobar, C. Perez Dengra, A. Pérez-Calero Yzquierdo, J. Puerta Pelayo, I. Redondo, L. Romero, S. Sánchez Navas, L. Urda Gómez, C. Willmott

Centro de Investigaciones Energéticas Medioambientales y Tecnológicas (CIEMAT), Madrid, Spain

J.F. de Trocóniz

Universidad Autónoma de Madrid, Madrid, Spain

B. Alvarez Gonzalez, J. Cuevas, C. Erice, J. Fernandez Menendez, S. Folgueras, I. Gonzalez Caballero, J.R. González Fernández, E. Palencia Cortezon, C. Ramón Álvarez, V. Rodríguez Bouza, A. Soto Rodríguez, A. Trapote, N. Trevisani, C. Vico Villalba

Universidad de Oviedo, Instituto Universitario de Ciencias y Tecnologías Espaciales de Asturias (ICTEA), Oviedo, Spain

J.A. Brochero Cifuentes, I.J. Cabrillo, A. Calderon, J. Duarte Campderros, M. Fernandez, C. Fernandez Madrazo, P.J. Fernández Manteca, A. García Alonso, G. Gomez, C. Martinez Rivero, P. Martinez Ruiz del Arbol, F. Matorras, P. Matorras Cuevas, J. Piedra Gomez, C. Prieels, A. Ruiz-Jimeno, L. Scodellaro, I. Vila, J.M. Vizan Garcia

Instituto de Física de Cantabria (IFCA), CSIC-Universidad de Cantabria, Santander, Spain

M.K. Jayananda, B. Kailasapathy⁵³, D.U.J. Sonnadara, D.D.C. Wickramarathna

University of Colombo, Colombo, Sri Lanka

W.G.D. Dharmaratna, K. Liyanage, N. Perera, N. Wickramage

University of Ruhuna, Department of Physics, Matara, Sri Lanka

T.K. Aarrestad, D. Abbaneo, J. Alimena, E. Auffray, G. Auzinger, J. Baechler, P. Baillon[†], D. Barney, J. Bendavid, M. Bianco, A. Bocci, C. Caillol, T. Camporesi, M. Capeans Garrido, G. Cerminara, N. Chernyavskaya, S.S. Chhibra, S. Choudhury, M. Cipriani, L. Cristella, D. d'Enterria, A. Dabrowski, A. David, A. De Roeck, M.M. Defranchis, M. Deile, M. Dobson, M. Dünser, N. Dupont, A. Elliott-Peisert, F. Fallavollita⁵⁴, A. Florent, L. Forthomme, G. Franzoni, W. Funk, S. Ghosh, S. Giani, D. Gigi, K. Gill, F. Glege, L. Gouskos, M. Haranko, J. Hegeman, V. Innocente, T. James, P. Janot, J. Kaspar, J. Kieseler, M. Komm, N. Kratochwil, C. Lange, S. Laurila, P. Lecoq, A. Lintuluoto, K. Long, C. Lourenço, B. Maier, L. Malgeri, S. Mallios, M. Mannelli, A.C. Marini, F. Meijers, S. Mersi, E. Meschi, F. Moortgat, M. Mulders, S. Orfanelli, L. Orsini, F. Pantaleo, E. Perez, M. Peruzzi, A. Petrilli, G. Petrucciani, A. Pfeiffer, M. Pierini, D. Piparo, M. Pitt, H. Qu, T. Quast, D. Rabad, A. Racz, G. Reales Gutiérrez, M. Rovere, H. Sakulin, J. Salfeld-Nebgen, S. Scarfi, C. Schäfer, M. Selvaggi, A. Sharma, P. Silva, W. Snoeys, P. Sphicas⁵⁵, S. Summers, K. Tatar, V.R. Tavolaro, D. Treille, P. Tropea, A. Tsiros, J. Wanczyk⁵⁶, K.A. Wozniak, W.D. Zeuner

CERN, European Organization for Nuclear Research, Geneva, Switzerland

L. Caminada⁵⁷, A. Ebrahimi, W. Erdmann, R. Horisberger, Q. Ingram, H.C. Kaestli, D. Kotlinski, M. Missiroli⁵⁷, L. Noehte⁵⁷, T. Rohe

Paul Scherrer Institut, Villigen, Switzerland

K. Androsov⁵⁶, M. Backhaus, P. Berger, A. Calandri, A. De Cosa, G. Dissertori, M. Dittmar, M. Donegà, C. Dorfer, F. Eble, K. Gedia, F. Glessgen, T.A. Gómez Espinosa, C. Grab, D. Hits, W. Lusteremann, A.-M. Lyon, R.A. Manzoni, L. Marchese, C. Martin Perez, M.T. Meinhard, F. Nessi-Tedaldi, J. Niedziela,

F. Pauss, V. Perovic, S. Pigazzini, M.G. Ratti, M. Reichmann, C. Reissel, T. Reitenspiess, B. Ristic, D. Ruini, D.A. Sanz Becerra, V. Stampf, J. Steggemann⁵⁶, R. Wallny

ETH Zurich – Institute for Particle Physics and Astrophysics (IPA), Zurich, Switzerland

C. Amsler⁵⁸, P. Bäertschi, C. Botta, D. Brzhechko, M.F. Canelli, K. Cormier, A. De Wit, R. Del Burgo, J.K. Heikkilä, M. Huwiler, W. Jin, A. Jofrehei, B. Kilminster, S. Leontsinis, S.P. Liechti, A. Macchiolo, P. Meiring, V.M. Mikuni, U. Molinatti, I. Neutelings, A. Reimers, P. Robmann, S. Sanchez Cruz, K. Schweiger, M. Senger, Y. Takahashi

Universität Zürich, Zurich, Switzerland

C. Adloff⁵⁹, C.M. Kuo, W. Lin, A. Roy, T. Sarkar³⁶, S.S. Yu

National Central University, Chung-Li, Taiwan

L. Ceard, Y. Chao, K.F. Chen, P.H. Chen, P.s. Chen, H. Cheng, W.-S. Hou, Y.y. Li, R.-S. Lu, E. Paganis, A. Psallidas, A. Steen, H.y. Wu, E. Yazgan, P.r. Yu

National Taiwan University (NTU), Taipei, Taiwan

B. Asavapibhop, C. Asawatangtrakuldee, N. Srimanobhas

Chulalongkorn University, Faculty of Science, Department of Physics, Bangkok, Thailand

F. Boran, S. Damarseckin⁶⁰, Z.S. Demiroglu, F. Dolek, I. Dumanoglu⁶¹, E. Eskut, Y. Guler⁶², E. Gurpinar Guler⁶², C. Isik, O. Kara, A. Kayis Topaksu, U. Kiminsu, G. Onengut, K. Ozdemir⁶³, A. Polatoz, A.E. Simsek, B. Tali⁶⁴, U.G. Tok, S. Turkcapar, I.S. Zorbakir

Çukurova University, Physics Department, Science and Art Faculty, Adana, Turkey

G. Karapinar, K. Ocalan⁶⁵, M. Yalvac⁶⁶

Middle East Technical University, Physics Department, Ankara, Turkey

B. Akgun, I.O. Atakisi, E. Gülmez, M. Kaya⁶⁷, O. Kaya⁶⁸, Ö. Özçelik, S. Tekten⁶⁹, E.A. Yetkin⁷⁰

Bogazici University, Istanbul, Turkey

A. Cakir, K. Cankocak⁶¹, Y. Komurcu, S. Sen⁷¹

Istanbul Technical University, Istanbul, Turkey

S. Cerci⁶⁴, I. Hos⁷², B. Isildak⁷³, B. Kaynak, S. Ozkorucuklu, H. Sert, C. Simsek, D. Sunar Cerci⁶⁴, C. Zorbilmez

Istanbul University, Istanbul, Turkey

B. Grynyov

Institute for Scintillation Materials of National Academy of Science of Ukraine, Kharkiv, Ukraine

L. Levchuk

National Science Centre, Kharkiv Institute of Physics and Technology, Kharkiv, Ukraine

D. Anthony, E. Bhal, S. Bologna, J.J. Brooke, A. Bundock, E. Clement, D. Cussans, H. Flacher, J. Goldstein, G.P. Heath, H.F. Heath, L. Kreczko, B. Krikler, S. Paramesvaran, S. Seif El Nasr-Storey, V.J. Smith, N. Stylianos⁷⁴, K. Walkingshaw Pass, R. White

University of Bristol, Bristol, United Kingdom

K.W. Bell, A. Belyaev⁷⁵, C. Brew, R.M. Brown, D.J.A. Cockerill, C. Cooke, K.V. Ellis, K. Harder, S. Harper, M.-L. Holmberg, J. Linacre, K. Manolopoulos, D.M. Newbold, E. Olaiya, D. Petyt, T. Reis, T. Schuh, C.H. Shepherd-Themistocleous, I.R. Tomalin, T. Williams

Rutherford Appleton Laboratory, Didcot, United Kingdom

R. Bainbridge, P. Bloch, S. Bonomally, J. Borg, S. Breeze, O. Buchmuller, V. Cepaitis, G.S. Chahal⁷⁶, D. Colling, P. Dauncey, G. Davies, M. Della Negra, S. Fayer, G. Fedi, G. Hall, M.H. Hassanshahi, G. Iles, J. Langford, L. Lyons, A.-M. Magnan, S. Malik, A. Martelli, D.G. Monk, J. Nash⁷⁷, M. Pesaresi, B.C. Radburn-Smith, D.M. Raymond, A. Richards, A. Rose, E. Scott, C. Seez, A. Shtipliyski, A. Tapper, K. Uchida, T. Virdee²⁰, M. Vojinovic, N. Wardle, S.N. Webb, D. Winterbottom

Imperial College, London, United Kingdom

K. Coldham, J.E. Cole, A. Khan, P. Kyberd, I.D. Reid, L. Teodorescu

Brunel University, Uxbridge, United Kingdom

S. Abdullin, A. Brinkerhoff, B. Caraway, J. Dittmann, K. Hatakeyama, A.R. Kanuganti, B. McMaster, N. Pastika, M. Saunders, S. Sawant, C. Sutantawibul, J. Wilson

Baylor University, Waco, TX, USA

R. Bartek, A. Dominguez, R. Uniyal, A.M. Vargas Hernandez

Catholic University of America, Washington, DC, USA

A. Buccilli, S.I. Cooper, D. Di Croce, S.V. Gleyzer, C. Henderson, C.U. Perez, P. Rumerio⁷⁸, C. West

The University of Alabama, Tuscaloosa, AL, USA

A. Akpinar, A. Albert, D. Arcaro, C. Cosby, Z. Demiragli, E. Fontanesi, D. Gastler, S. May, J. Rohlf, K. Salyer, D. Sperka, D. Spitzbart, I. Suarez, A. Tsatsos, S. Yuan, D. Zou

Boston University, Boston, MA, USA

G. Benelli, B. Burkle, X. Coubez²¹, D. Cutts, M. Hadley, U. Heintz, J.M. Hogan⁷⁹, T. Kwon, G. Landsberg, K.T. Lau, D. Li, M. Lukasik, J. Luo, M. Narain, N. Pervan, S. Sagir⁸⁰, F. Simpson, E. Usai, W.Y. Wong, X. Yan, D. Yu, W. Zhang

Brown University, Providence, RI, USA

J. Bonilla, C. Brainerd, R. Breedon, M. Calderon De La Barca Sanchez, M. Chertok, J. Conway, P.T. Cox, R. Erbacher, G. Haza, F. Jensen, O. Kukral, R. Lander, M. Mulhearn, D. Pellett, B. Regnery, D. Taylor, Y. Yao, F. Zhang

University of California, Davis, Davis, CA, USA

M. Bachtis, R. Cousins, A. Datta, D. Hamilton, J. Hauser, M. Ignatenko, M.A. Iqbal, T. Lam, W.A. Nash, S. Regnard, D. Saltzberg, B. Stone, V. Valuev

University of California, Los Angeles, CA, USA

Y. Chen, R. Clare, J.W. Gary, M. Gordon, G. Hanson, G. Karapostoli, O.R. Long, N. Manganeli, W. Si, S. Wimpenny, Y. Zhang

University of California, Riverside, Riverside, CA, USA

J.G. Branson, P. Chang, S. Cittolin, S. Cooperstein, N. Deelen, D. Diaz, J. Duarte, R. Gerosa, L. Giannini, J. Guiang, R. Kansal, V. Krutelyov, R. Lee, J. Letts, M. Masciovecchio, F. Mokhtar, M. Pieri, B.V. Sathia Narayanan, V. Sharma, M. Tadel, F. Würthwein, Y. Xiang, A. Yagil

University of California, San Diego, La Jolla, CA, USA

N. Amin, C. Campagnari, M. Citron, G. Collura, A. Dorsett, V. Dutta, J. Incandela, M. Kilpatrick, J. Kim, B. Marsh, H. Mei, M. Oshiro, M. Quinnan, J. Richman, U. Sarica, F. Setti, J. Sheplock, P. Siddireddy, D. Stuart, S. Wang

University of California, Santa Barbara – Department of Physics, Santa Barbara, CA, USA

A. Bornheim, O. Cerri, I. Dutta, J.M. Lawhorn, N. Lu, J. Mao, H.B. Newman, T.Q. Nguyen, M. Spiropulu, J.R. Vlimant, C. Wang, S. Xie, Z. Zhang, R.Y. Zhu

California Institute of Technology, Pasadena, CA, USA

J. Alison, S. An, M.B. Andrews, P. Bryant, T. Ferguson, A. Harilal, C. Liu, T. Mudholkar, M. Paulini, A. Sanchez, W. Terrill

Carnegie Mellon University, Pittsburgh, PA, USA

J.P. Cumalat, W.T. Ford, A. Hassani, G. Karathanasis, E. MacDonald, R. Patel, A. Perloff, C. Savard, N. Schonbeck, K. Stenson, K.A. Ulmer, S.R. Wagner, N. Zipper

University of Colorado Boulder, Boulder, CO, USA

J. Alexander, S. Bright-Thonney, X. Chen, Y. Cheng, D.J. Cranshaw, S. Hogan, J. Monroy, J.R. Patterson, D. Quach, J. Reichert, M. Reid, A. Ryd, W. Sun, J. Thom, P. Wittich, R. Zou

Cornell University, Ithaca, NY, USA

M. Albrow, M. Alyari, G. Apollinari, A. Apresyan, A. Apyan, L.A.T. Bauerdick, D. Berry, J. Berryhill, P.C. Bhat, K. Burkett, J.N. Butler, A. Canepa, G.B. Cerati, H.W.K. Cheung, F. Chlebana, K.F. Di Petrillo, J. Dickinson, V.D. Elvira, Y. Feng, J. Freeman, Z. Gecse, L. Gray, D. Green, S. Grünendahl, O. Gutsche, R.M. Harris, R. Heller, T.C. Herwig, J. Hirschauer, B. Jayatilaka, S. Jindariani, M. Johnson, U. Joshi, T. Klijsma, B. Klima, K.H.M. Kwok, S. Lammel, D. Lincoln, R. Lipton, T. Liu, C. Madrid, K. Maeshima, C. Mantilla, D. Mason, P. McBride, P. Merkel, S. Mrenna, S. Nahn, J. Ngadiuba, V. Papadimitriou, K. Pedro, C. Pena⁸¹, F. Ravera, A. Reinsvold Hall⁸², L. Ristori, E. Sexton-Kennedy, N. Smith, A. Soha, L. Spiegel, J. Strait, L. Taylor, S. Tkaczyk, N.V. Tran, L. Uplegger, E.W. Vaandering, H.A. Weber

Fermi National Accelerator Laboratory, Batavia, IL, USA

P. Avery, D. Bourilkov, L. Cadamuro, V. Cherepanov, R.D. Field, D. Guerrero, B.M. Joshi, M. Kim, E. Koenig, J. Konigsberg, A. Korytov, K.H. Lo, K. Matchev, N. Menendez, G. Mitselmakher, A. Muthirakalayil Madhu, N. Rawal, D. Rosenzweig, S. Rosenzweig, K. Shi, J. Wang, Z. Wu, E. Yigitbasi, X. Zuo

University of Florida, Gainesville, FL, USA

T. Adams, A. Askew, R. Habibullah, V. Hagopian, K.F. Johnson, R. Khurana, T. Kolberg, G. Martinez, H. Prosper, C. Schiber, O. Viazlo, R. Yohay, J. Zhang

Florida State University, Tallahassee, FL, USA

M.M. Baarmand, S. Butalla, T. Elkafrawy⁸³, M. Hohlmann, R. Kumar Verma, D. Noonan, M. Rahmani, F. Yumiceva

Florida Institute of Technology, Melbourne, FL, USA

M.R. Adams, H. Becerril Gonzalez, R. Cavanaugh, S. Dittmer, O. Evdokimov, C.E. Gerber, D.J. Hofman, A.H. Merrit, C. Mills, G. Oh, T. Roy, S. Rudrabhatla, M.B. Tonjes, N. Varelas, J. Viinikainen, X. Wang, Z. Ye

University of Illinois at Chicago (UIC), Chicago, IL, USA

M. Alhusseini, K. Dilsiz⁸⁴, L. Emediato, R.P. Gandrajula, O.K. Köseyan, J.-P. Merlo, A. Mestvirishvili⁸⁵, J. Nachtman, H. Ogul⁸⁶, Y. Onel, A. Penzo, C. Snyder, E. Tiras⁸⁷

The University of Iowa, Iowa City, IA, USA

O. Amram, B. Blumenfeld, L. Corcodilos, J. Davis, A.V. Gritsan, S. Kyriacou, P. Maksimovic, J. Roskes, M. Swartz, T.Á. Vámi

Johns Hopkins University, Baltimore, MD, USA

A. Abreu, J. Anguiano, C. Baldenegro Barrera, P. Baringer, A. Bean, Z. Flowers, T. Isidori, S. Khalil, J. King, G. Krintiras, A. Kropivnitskaya, M. Lazarovits, C. Le Mahieu, C. Lindsey, J. Marquez, N. Minafra, M. Murray, M. Nickel, C. Rogan, C. Royon, R. Salvatico, S. Sanders, E. Schmitz, C. Smith, Q. Wang, Z. Warner, J. Williams, G. Wilson

The University of Kansas, Lawrence, KS, USA

S. Duric, A. Ivanov, K. Kaadze, D. Kim, Y. Maravin, T. Mitchell, A. Modak, K. Nam

Kansas State University, Manhattan, KS, USA

F. Rebassoo, D. Wright

Lawrence Livermore National Laboratory, Livermore, CA, USA

E. Adams, A. Baden, O. Baron, A. Belloni, S.C. Eno, N.J. Hadley, S. Jabeen, R.G. Kellogg, T. Koeth, Y. Lai, S. Lascio, A.C. Mignerey, S. Nabili, C. Palmer, M. Seidel, A. Skuja, L. Wang, K. Wong

University of Maryland, College Park, MD, USA

D. Abercrombie, G. Andreassi, R. Bi, W. Busza, I.A. Cali, Y. Chen, M. D'Alfonso, J. Eysermans, C. Freer, G. Gomez-Ceballos, M. Goncharov, P. Harris, M. Hu, M. Klute, D. Kovalskyi, J. Krupa, Y.-J. Lee, C. Mironov, C. Paus, D. Rankin, C. Roland, G. Roland, Z. Shi, G.S.F. Stephans, J. Wang, Z. Wang, B. Wyslouch

Massachusetts Institute of Technology, Cambridge, MA, USA

R.M. Chatterjee, A. Evans, J. Hiltbrand, Sh. Jain, M. Krohn, Y. Kubota, J. Mans, M. Revering, R. Rusack, R. Saradhy, N. Schroeder, N. Strobbe, M.A. Wadud

University of Minnesota, Minneapolis, MN, USA

K. Bloom, M. Bryson, S. Chauhan, D.R. Claes, C. Fangmeier, L. Finco, F. Golf, C. Joo, I. Kravchenko, I. Reed, J.E. Siado, G.R. Snow[†], W. Tabb, A. Wightman, F. Yan, A.G. Zecchinelli

University of Nebraska-Lincoln, Lincoln, NE, USA

G. Agarwal, H. Bandyopadhyay, L. Hay, I. Iashvili, A. Kharchilava, C. McLean, D. Nguyen, J. Pekkanen, S. Rappoccio, A. Williams

State University of New York at Buffalo, Buffalo, NY, USA

G. Alverson, E. Barberis, Y. Haddad, Y. Han, A. Hortiangtham, A. Krishna, J. Li, J. Lidrych, G. Madigan, B. Marzocchi, D.M. Morse, V. Nguyen, T. Orimoto, A. Parker, L. Skinnari, A. Tishelman-Charny, T. Wamorkar, B. Wang, A. Wisecarver, D. Wood

Northeastern University, Boston, MA, USA

S. Bhattacharya, J. Bueghly, Z. Chen, A. Gilbert, T. Gunter, K.A. Hahn, Y. Liu, N. Odell, M.H. Schmitt, M. Velasco

Northwestern University, Evanston, IL, USA

R. Band, R. Bucci, M. Cremonesi, A. Das, N. Dev, R. Goldouzian, M. Hildreth, K. Hurtado Anampa, C. Jessop, K. Lannon, J. Lawrence, N. Loukas, L. Lutton, J. Mariano, N. Marinelli, I. Mcalister, T. McCauley, C. Mcgrady, K. Mohrman, C. Moore, Y. Musienko¹³, R. Ruchti, A. Townsend, M. Wayne, M. Zarucki, L. Zygala

University of Notre Dame, Notre Dame, IN, USA

B. Bylsma, L.S. Durkin, B. Francis, C. Hill, M. Nunez Ornelas, K. Wei, B.L. Winer, B.R. Yates

The Ohio State University, Columbus, OH, USA

F.M. Addesa, B. Bonham, P. Das, G. Dezoort, P. Elmer, A. Frankenthal, B. Greenberg, N. Haubrich, S. Higginbotham, A. Kalogeropoulos, G. Kopp, S. Kwan, D. Lange, D. Marlow, K. Mei, I. Ojalvo, J. Olsen, D. Stickland, C. Tully

Princeton University, Princeton, NJ, USA

S. Malik, S. Norberg

University of Puerto Rico, Mayaguez, PR, USA

A.S. Bakshi, V.E. Barnes, R. Chawla, S. Das, L. Gutay, M. Jones, A.W. Jung, D. Kondratyev, A.M. Koshy, M. Liu, G. Negro, N. Neumeister, G. Paspalaki, S. Piperov, A. Purohit, J.F. Schulte, M. Stojanovic, J. Thieman, F. Wang, R. Xiao, W. Xie

Purdue University, West Lafayette, IN, USA

J. Dolen, N. Parashar

Purdue University Northwest, Hammond, IN, USA

D. Acosta, A. Baty, T. Carnahan, M. Decaro, S. Dildick, K.M. Ecklund, S. Freed, P. Gardner, F.J.M. Geurts, A. Kumar, W. Li, B.P. Padley, R. Redjimi, J. Rotter, W. Shi, A.G. Stahl Leiton, S. Yang, L. Zhang⁸⁸, Y. Zhang

Rice University, Houston, TX, USA

A. Bodek, P. de Barbaro, R. Demina, J.L. Dulemba, C. Fallon, T. Ferbel, M. Galanti, A. Garcia-Bellido, O. Hindrichs, A. Khukhunaishvili, E. Ranken, R. Taus, G.P. Van Onsem

University of Rochester, Rochester, NY, USA

B. Chiarito, J.P. Chou, A. Gandrakota, Y. Gershtein, E. Halkiadakis, A. Hart, M. Heindl, O. Karacheban²⁴, I. Laflotte, A. Lath, R. Montalvo, K. Nash, M. Osherson, S. Salur, S. Schnetzer, S. Somalwar, R. Stone, S.A. Thayil, S. Thomas, H. Wang

Rutgers, The State University of New Jersey, Piscataway, NJ, USA

H. Acharya, A.G. Delannoy, S. Fiorendi, S. Spanier

University of Tennessee, Knoxville, TN, USA

O. Bouhali⁸⁹, M. Dalchenko, A. Delgado, R. Eusebi, J. Gilmore, T. Huang, T. Kamon⁹⁰, H. Kim, S. Luo, S. Malhotra, R. Mueller, D. Overton, D. Rathjens, A. Safonov

Texas A&M University, College Station, TX, USA

N. Akchurin, J. Damgov, V. Hegde, S. Kunori, K. Lamichhane, S.W. Lee, T. Mengke, S. Muthumuni, T. Peltola, I. Volobouev, Z. Wang, A. Whitbeck

Texas Tech University, Lubbock, TX, USA

E. Appelt, S. Greene, A. Gurrola, W. Johns, A. Melo, K. Padeken, F. Romeo, P. Sheldon, S. Tuo, J. Velkovska

Vanderbilt University, Nashville, TN, USA

M.W. Arenton, B. Cardwell, B. Cox, G. Cummings, J. Hakala, R. Hirosky, M. Joyce, A. Ledovskoy, A. Li, C. Neu, C.E. Perez Lara, B. Tannenwald, S. White

University of Virginia, Charlottesville, VA, USA

N. Poudyal

Wayne State University, Detroit, MI, USA

S. Banerjee, K. Black, T. Bose, S. Dasu, I. De Bruyn, P. Everaerts, C. Galloni, H. He, M. Herndon, A. Herve, U. Hussain, A. Lanaro, A. Loeliger, R. Loveless, J. Madhusudanan Sreekala, A. Mallampalli, A. Mohammadi, D. Pinna, A. Savin, V. Shang, V. Sharma, W.H. Smith, D. Teague, S. Trembath-Reichert, W. Vetens

University of Wisconsin – Madison, Madison, WI, USA

S. Afanasiev, V. Andreev, Yu. Andreev, T. Aushev, M. Azarkin, A. Babaev, A. Belyaev, V. Blinov⁹¹, E. Boos, V. Borshch, D. Budkouski, O. Bychkova, M. Chadeeva⁹¹, V. Chekhovsky, A. Dermenev, T. Dimova⁹¹, I. Dremin, M. Dubinin⁸¹, L. Dudko, V. Epshteyn, A. Ershov, G. Gavrillov, V. Gavrillov, S. Gninenko, V. Golovtsov, N. Golubev, I. Golutvin, I. Gorbunov, A. Gribushin, V. Ivanchenko, Y. Ivanov, V. Kachanov, L. Kardapoltsev⁹¹, V. Karjavine, A. Karneyeu, V. Kim⁹¹, M. Kirakosyan, D. Kirpichnikov, M. Kirsanov, V. Klyukhin, O. Kodolova⁹², D. Konstantinov, V. Korenkov, A. Kozyrev⁹¹, N. Krasnikov, E. Kuznetsova⁹³, A. Lanev, A. Litomin, N. Lychkovskaya, V. Makarenko, A. Malakhov, V. Matveev⁹¹, V. Murzin, A. Nikitenko⁹⁴, S. Obraztsov, V. Okhotnikov, V. Oreshkin, A. Oskin, I. Ovtin⁹¹, V. Palichik, P. Parygin, A. Pashenkov, V. Perelygin, S. Petrushanko, G. Pivovarov, V. Popov, E. Popova, O. Radchenko⁹¹, V. Rusinov, M. Savina, V. Savrin, V. Shalaev, S. Shmatov, S. Shulha, Y. Skovpen⁹¹, S. Slabospitskii, I. Smirnov, V. Smirnov, A. Snigirev, D. Sosnov, A. Stepenov, V. Sulimov, E. Tcherniaev, A. Terkulov, O. Teryaev, M. Toms, A. Toropin, L. Uvarov, A. Uzunian, E. Vlasov, S. Volkov, A. Vorobyev, N. Voytishin, B.S. Yuldashev⁹⁵, A. Zarubin, I. Zhizhin, A. Zhokin

Authors affiliated with an institute or an international laboratory covered by a cooperation agreement with CERN

† Deceased.

¹ Also at Yerevan State University, Yerevan, Armenia.

² Also at TU Wien, Vienna, Austria.

³ Also at Institute of Basic and Applied Sciences, Faculty of Engineering, Arab Academy for Science, Technology and Maritime Transport, Alexandria, Egypt.

⁴ Also at Université Libre de Bruxelles, Bruxelles, Belgium.

⁵ Also at Universidade Estadual de Campinas, Campinas, Brazil.

⁶ Also at Federal University of Rio Grande do Sul, Porto Alegre, Brazil.

⁷ Also at The University of the State of Amazonas, Manaus, Brazil.

⁸ Also at University of Chinese Academy of Sciences, Beijing, China.

⁹ Also at UFMS, Nova Andradina, Brazil.

¹⁰ Also at Nanjing Normal University Department of Physics, Nanjing, China.

¹¹ Now at The University of Iowa, Iowa City, Iowa, USA.

¹² Also at University of Chinese Academy of Sciences, Beijing, China.

¹³ Also at an institute or an international laboratory covered by a cooperation agreement with CERN.

¹⁴ Also at Cairo University, Cairo, Egypt.

¹⁵ Also at Zewail City of Science and Technology, Zewail, Egypt.

¹⁶ Also at Purdue University, West Lafayette, Indiana, USA.

¹⁷ Also at Université de Haute Alsace, Mulhouse, France.

¹⁸ Also at Tbilisi State University, Tbilisi, Georgia.

¹⁹ Also at Erzincan Binali Yildirim University, Erzincan, Turkey.

²⁰ Also at CERN, European Organization for Nuclear Research, Geneva, Switzerland.

²¹ Also at RWTH Aachen University, III. Physikalisches Institut A, Aachen, Germany.

²² Also at University of Hamburg, Hamburg, Germany.

²³ Also at Isfahan University of Technology, Isfahan, Iran.

²⁴ Also at Brandenburg University of Technology, Cottbus, Germany.

²⁵ Also at Forschungszentrum Jülich, Juelich, Germany.

²⁶ Also at Physics Department, Faculty of Science, Assiut University, Assiut, Egypt.

²⁷ Also at Karoly Robert Campus, MATE Institute of Technology, Gyongyos, Hungary.

²⁸ Also at Institute of Physics, University of Debrecen, Debrecen, Hungary.

²⁹ Also at Institute of Nuclear Research ATOMKI, Debrecen, Hungary.

³⁰ Now at Universitatea Babeş-Bolyai – Facultatea de Fizica, Cluj-Napoca, Romania.

³¹ Also at MTA-ELTE Lendület CMS Particle and Nuclear Physics Group, Eötvös Loránd University, Budapest, Hungary.

³² Also at Wigner Research Centre for Physics, Budapest, Hungary.

³³ Also at Punjab Agricultural University, Ludhiana, India.

³⁴ Also at Shoolini University, Solan, India.

³⁵ Also at University of Hyderabad, Hyderabad, India.

³⁶ Also at University of Visva-Bharati, Santiniketan, India.

³⁷ Also at Indian Institute of Science (IISc), Bangalore, India.

³⁸ Also at Indian Institute of Technology (IIT), Mumbai, India.

³⁹ Also at IIT Bhubaneswar, Bhubaneswar, India.

⁴⁰ Also at Institute of Physics, Bhubaneswar, India.

⁴¹ Also at Deutsches Elektronen-Synchrotron, Hamburg, Germany.

⁴² Also at Sharif University of Technology, Tehran, Iran.

⁴³ Also at Department of Physics, University of Science and Technology of Mazandaran, Behshahr, Iran.

- ⁴⁴ Also at Helwan University, Cairo, Egypt.
- ⁴⁵ Also at Italian National Agency for New Technologies, Energy and Sustainable Economic Development, Bologna, Italy.
- ⁴⁶ Also at Centro Siciliano di Fisica Nucleare e di Struttura Della Materia, Catania, Italy.
- ⁴⁷ Also at Scuola Superiore Meridionale, Università di Napoli 'Federico II', Napoli, Italy.
- ⁴⁸ Also at Università di Napoli 'Federico II', Napoli, Italy.
- ⁴⁹ Also at Consiglio Nazionale delle Ricerche – Istituto Officina dei Materiali, Perugia, Italy.
- ⁵⁰ Also at Consejo Nacional de Ciencia y Tecnología, Mexico City, Mexico.
- ⁵¹ Also at IRFU, CEA, Université Paris-Saclay, Gif-sur-Yvette, France.
- ⁵² Also at Faculty of Physics, University of Belgrade, Belgrade, Serbia.
- ⁵³ Also at Trincomalee Campus, Eastern University, Sri Lanka, Nilaveli, Sri Lanka.
- ⁵⁴ Also at INFN Sezione di Pavia, Università di Pavia, Pavia, Italy.
- ⁵⁵ Also at National and Kapodistrian University of Athens, Athens, Greece.
- ⁵⁶ Also at Ecole Polytechnique Fédérale Lausanne, Lausanne, Switzerland.
- ⁵⁷ Also at Universität Zürich, Zurich, Switzerland.
- ⁵⁸ Also at Stefan Meyer Institute for Subatomic Physics, Vienna, Austria.
- ⁵⁹ Also at Laboratoire d'Annecy-le-Vieux de Physique des Particules, IN2P3-CNRS, Annecy-le-Vieux, France.
- ⁶⁰ Also at Şırnak University, Şırnak, Turkey.
- ⁶¹ Also at Near East University, Research Center of Experimental Health Science, Mersin, Turkey.
- ⁶² Also at Konya Technical University, Konya, Turkey.
- ⁶³ Also at Izmir Bakircay University, Izmir, Turkey.
- ⁶⁴ Also at Adiyaman University, Adiyaman, Turkey.
- ⁶⁵ Also at Necmettin Erbakan University, Konya, Turkey.
- ⁶⁶ Also at Bozok Universitetesi Rektörlüğü, Yozgat, Turkey.
- ⁶⁷ Also at Marmara University, Istanbul, Turkey.
- ⁶⁸ Also at Milli Savunma University, Istanbul, Turkey.
- ⁶⁹ Also at Kafkas University, Kars, Turkey.
- ⁷⁰ Also at Istanbul Bilgi University, Istanbul, Turkey.
- ⁷¹ Also at Hacettepe University, Ankara, Turkey.
- ⁷² Also at Istanbul University – Cerrahpasa, Faculty of Engineering, Istanbul, Turkey.
- ⁷³ Also at Yildiz Technical University, Istanbul, Turkey.
- ⁷⁴ Also at Vrije Universiteit Brussel, Brussel, Belgium.
- ⁷⁵ Also at School of Physics and Astronomy, University of Southampton, Southampton, United Kingdom.
- ⁷⁶ Also at IPPP Durham University, Durham, United Kingdom.
- ⁷⁷ Also at Monash University, Faculty of Science, Clayton, Australia.
- ⁷⁸ Also at Università di Torino, Torino, Italy.
- ⁷⁹ Also at Bethel University, St. Paul, Minnesota, USA.
- ⁸⁰ Also at Karamanoğlu Mehmetbey University, Karaman, Turkey.
- ⁸¹ Also at California Institute of Technology, Pasadena, California, USA.
- ⁸² Also at United States Naval Academy, Annapolis, Maryland, USA.
- ⁸³ Also at Ain Shams University, Cairo, Egypt.
- ⁸⁴ Also at Bingol University, Bingol, Turkey.
- ⁸⁵ Also at Georgian Technical University, Tbilisi, Georgia.
- ⁸⁶ Also at Sinop University, Sinop, Turkey.
- ⁸⁷ Also at Erciyes University, Kayseri, Turkey.
- ⁸⁸ Also at Institute of Modern Physics and Key Laboratory of Nuclear Physics and Ion-beam Application (MOE) – Fudan University, Shanghai, China.
- ⁸⁹ Also at Texas A&M University at Qatar, Doha, Qatar.
- ⁹⁰ Also at Kyungpook National University, Daegu, Republic of Korea.
- ⁹¹ Also at another institute or international laboratory covered by a cooperation agreement with CERN.
- ⁹² Also at Yerevan Physics Institute, Yerevan, Armenia.
- ⁹³ Also at University of Florida, Gainesville, Florida, USA.
- ⁹⁴ Also at Imperial College, London, United Kingdom.
- ⁹⁵ Also at Institute of Nuclear Physics of the Uzbekistan Academy of Sciences, Tashkent, Uzbekistan.